

贺根山缝合带晚石炭世 TTG 岩浆事件： 奥长花岗岩锆石 U-Pb 年龄和地球化学制约

王金芳, 李英杰, 李红阳, 董培培

河北地质大学地球科学学院, 石家庄, 050031

内容提要:本文以贺根山缝合带呼都格奥长花岗岩体为研究对象, 通过野外地质调查和岩石学、地球化学、锆石 U-Pb 年代学研究, 讨论岩石成因、构造环境、TTG 岩浆事件及古亚洲洋俯冲消亡过程。岩石地球化学研究表明, 呼都格岩体富硅 ($\text{SiO}_2 = 66.27\% \sim 71.59\%$)、高铝 ($\text{Al}_2\text{O}_3 = 15.23\% \sim 15.94\%$)、富钠 ($\text{Na}_2\text{O} = 4.13\% \sim 6.59\%$)、低钾 ($\text{K}_2\text{O} = 1.72\% \sim 2.53\%$), 相对高锶 ($\text{Sr} = 196.60 \times 10^{-6} \sim 465.40 \times 10^{-6}$)、低钇 ($\text{Y} = 5.70 \times 10^{-6} \sim 12.63 \times 10^{-6}$), 富集 Ba、Sr 等大离子亲石元素和 LREE, 亏损 Nb、Ta、Ti、P 等高场强元素和 HREE, 无明显 Eu 异常。岩石学和岩石地球化学特征表明, 呼都格岩体属于以奥长花岗岩为主的英云闪长岩-奥长花岗岩-花岗闪长岩 TTG 岩石组合。这套 TTG 组合除 Sr、Mg、Ni 和 Cr 含量相对较低之外, 与高 Si 埃达克岩的地球化学特征相类似, 形成于大洋俯冲带岛弧环境, 可能为俯冲洋壳脱水熔融成因。锆石 LA-ICP-MS U-Pb 测年获得两组年龄为 $306.3 \pm 1.9\text{ Ma}$ 和 $315.5 \pm 1.9\text{ Ma}$, 表明该岩体侵位于晚石炭世, 反映了贺根山缝合带晚石炭世大洋俯冲带 TTG 岩浆事件。结合其与梅劳特乌拉-高力罕蛇绿岩-TTG 岩带前弧玄武岩、高镁安山岩/高镁闪长岩、埃达克岩、TTG、富铌弧玄武岩/辉长岩的岩石构造组合, 认为古亚洲洋二连-贺根山洋盆在晚石炭世可能处于洋壳俯冲消减、TTG 岩浆活动和新生陆壳生长洋陆转换过程中。

关键词:奥长花岗岩; TTG; 晚石炭世; 洋陆转换; 贺根山缝合带

二连-贺根山缝合带是中亚增生型造山带东段华北陆块北缘增生带的典型代表之一, 保留了大量洋壳俯冲消减与新生陆壳生长等古亚洲洋构造演化信息, 涉及到造山带的增生机制、形成过程、构造演化等洋陆转换关键科学问题, 成为探讨与研究古亚洲洋如何通过洋陆转换形成中亚增生型造山带的重要热点区域之一 (Sengor et al., 1993; Chen Bin et al., 2000; Xiao Wenjiao et al., 2003; Windley et al., 2007; Miao Laicheng et al., 2008; Jian Ping et al., 2010; Liu Jianfeng et al., 2013; Deng Jinfu et al., 2015b; Safonova, 2017; Wang Shuqing et al., 2018; Cheng Yang et al., 2019, 2020)。而作为地壳重要物质成分的英云闪长岩-奥长花岗岩-花岗闪长岩 (TTG) 岩类, 既广泛分布于太古宙—古元古代花岗-绿岩带, 亦是显生宙增生型造山带 (大洋俯冲带)

的重要岩石组成。虽然 TTG 的成因长期存在着俯冲洋壳部分熔融与加厚镁铁质下地壳部分熔融“板块”与“非板块”两种主要观点 (Martin, 1987, 1999; Rapp et al., 1991, 1995, 2003; Foley et al., 2002, 2003; Martin et al., 2005; Condie, 2005; Hawkesworth et al., 2010; Adam et al., 2012), 但是地球化学与实验岩石学研究已经证实 TTG 形成于含水玄武质岩石在石榴角闪岩相或榴辉岩相的部分熔融 (Condie, 1986; Martin, 1999; Foley et al., 2002; Rapp et al., 2003)。而且人们普遍认为显生宙 TTG 组合是形成于大洋俯冲带岛弧环境的典型火成岩构造组合, 为大洋俯冲玄武岩板片脱水熔融的产物 (Rapp et al., 1995; Drummond et al., 1996; Foley et al., 2003; Martin et al., 2005; Wu Mingqian et al., 2014; Deng Jinfu et al., 2015a,

注: 本文为国家自然科学基金(编号 41972061、41502211)和中国地质调查局“内蒙古 1:5 万高力罕牧场三连等四幅区调”(编号 1212011120711)项目资助的成果。

收稿日期: 2019-09-06; 改回日期: 2020-05-27; 网络发表日期: 2021-01-14; 责任编委: 吴才来; 责任编辑: 李曼。

作者简介: 王金芳, 女, 1983 年生。副教授, 主要从事岩石学和地球化学研究。Email: wjfb1983@163.com。

引用本文: 王金芳, 李英杰, 李红阳, 董培培. 2021. 贺根山缝合带晚石炭世 TTG 岩浆事件: 奥长花岗岩锆石 U-Pb 年龄和地球化学制约地
质学报, 95(2): 396~412, doi: 10.19762/j.cnki.dizhixuebao.2021204.

Wang Jinfang, Li Yingjie, Li Hongyang, Dong Peipei. 2021. Late Carboniferous TTG magmatic event in the Hegenshan suture zone: zircon U-Pb geochronology and geochemical constraints from the Huduge trondhjemite. Acta Geologica Sinica, 95(2): 396~412.

2018; Xue Jianping et al., 2018),是造山带地壳增生与构造演化的重要岩石记录。大量研究表明,显生宙的 TTG 岩浆事件是新生陆壳生长的重要地质作用,英云闪长岩-奥长花岗岩-花岗闪长岩(TTG)组合的出现代表了新生陆壳生长事件或陆壳的增生,并在大陆雏体形成中具有重要意义,也是表征显生宙增生型造山带的增生与洋陆转换的关键所在。因此,TTG 岩石成因、构造环境、形成时代的研究,可为增生型造山带新生陆壳的形成、增生机制、构造演化提供重要的岩石学、年代学和地球化学依据。

近十年来,针对古亚洲洋二连-贺根山洋盆俯冲构造岩浆事件典型火成岩构造组合开展了大量的野外地质调查和岩石学、地球化学、锆石 U-Pb 年代学等研究,在二连-贺根山缝合带区域内识别出许多石炭纪一二叠纪 SSZ 型蛇绿岩和岛弧型岩浆岩,厘定出二连-贺根山洋晚古生代大洋俯冲作用与新生陆壳生长构造岩浆事件(Miao Laicheng et al., 2008; Chen Bin et al., 2009; Xiao Wenjiao et al., 2009; Jian Ping et al., 2010, 2012; Liu Jianfeng et al., 2009, 2013; Shi Yuruo et al., 2014; Deng Jinfu et al., 2015b; Liu Rui et al., 2016; Safonova, 2017;

Wang Shuqing et al., 2018; Cheng Yang et al., 2019, 2020)。尤其是近几年,新识别的梅劳特乌拉-高力罕蛇绿岩-TTG 岩带和迪彦庙蛇绿岩带的前弧玄武岩、高镁安山岩/高镁闪长岩-镁安山岩、埃达克岩、TTG、富铌弧玄武岩/辉长岩等洋内弧火成岩构造组合,初步厘定出二连-贺根山缝合带区域内以梅劳特乌拉和迪彦庙洋内弧为代表的石炭纪一二叠纪洋内俯冲构造岩浆事件(图 1,2),蕴涵着二连-贺根山洋可能普遍存在洋内俯冲作用与洋内弧的重要信息(Li Yingjie et al., 2012, 2015, 2018a, 2018b, 2018c; Wang Cheng et al., 2019; Wang Jinfang et al., 2017a, 2017c, 2018a, 2018b, 2019a, 2020a, 2020b; Cheng Yang et al., 2019, 2020)。而这些岛弧岩浆岩,特别是洋内弧或洋内弧火成岩构造组合所形成的弧地壳或大陆雏体,记录着古亚洲洋洋壳俯冲消减作用、TTG 岩浆作用和新生陆壳生长等洋陆转化过程信息。因此,与梅劳特乌拉洋内弧密切共生的呼都格奥长花岗岩体的研究,对于识别古亚洲洋晚古生代大洋俯冲、TTG 岩浆活动和新生陆壳生长等构造岩浆事件具有重要意义。

然而,中亚造山带东段古亚洲洋的最终闭合时

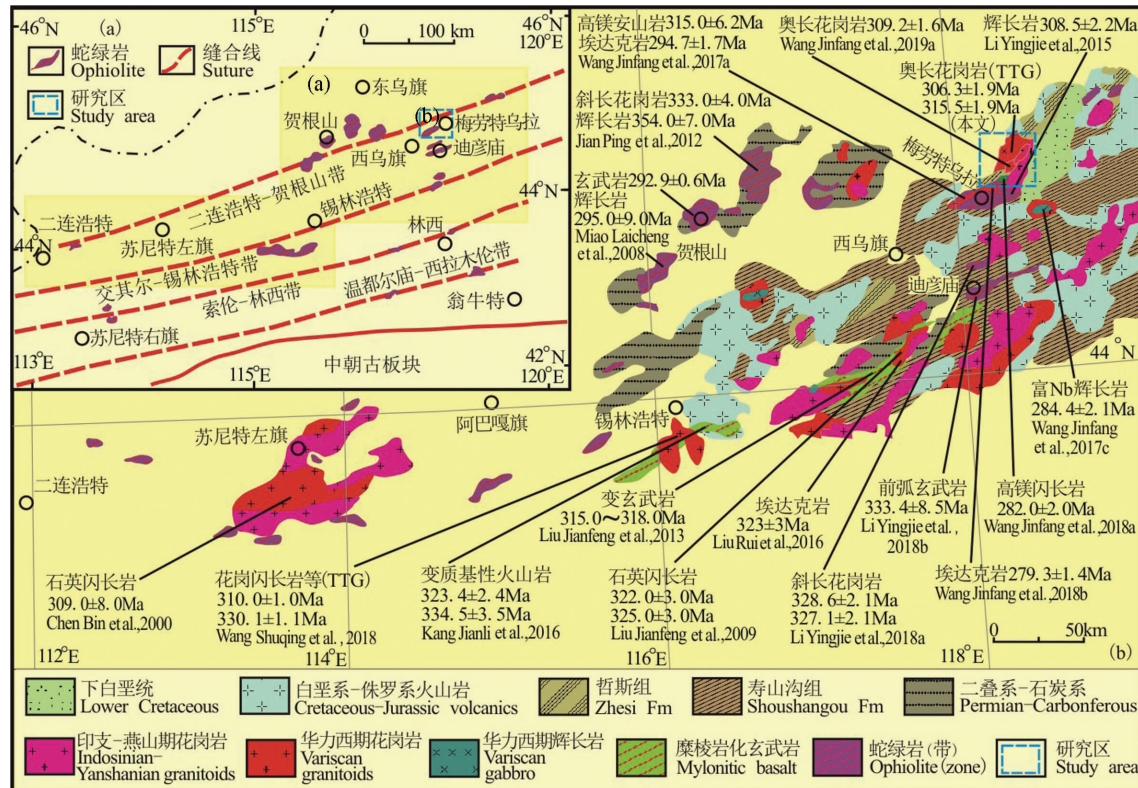


图 1 二连-贺根山缝合带区域构造(a)(据 Miao Laicheng et al., 2008)与区域地质简图(b)

Fig. 1 Sketch tectonic map (a) (modified from Miao Laicheng et al., 2008) and regional geological map (b) of the Erenhot-Hegenshan suture zone

间问题,长期存在着“晚二叠世”和“晚泥盆世”两种主要观点与争议,在一定程度上制约着二连-贺根山缝合带构造演化的研究与认识。虽然,古亚洲洋“晚二叠世最终闭合”已是一种主流观点(Chen Bin et al., 2001, 2009; Xiao Wenjiao et al., 2003, 2009; Li Jinyi et al., 2007; Miao Laicheng et al., 2008; Jian Ping et al., 2010, 2012; Liu Jianfeng et al., 2009, 2013; Deng Jinfu et al., 2015b; Kang Jianli et al., 2016; Zhang Xiaofei et al., 2018; Fan Yuxu et al., 2019; Cheng Yang et al., 2019, 2020),但是,与该区石炭纪 SSZ 型蛇绿岩和洋内弧密切共生的晚石炭世奥长花岗岩体尚未见有报道,古亚洲洋二连-贺根山洋盆晚石炭世俯冲作用与“晚二叠世”闭合时间仍需要进一步的大洋俯冲构造岩浆事件与岛弧岩浆岩石学证据及年代学约束。笔者在近年内蒙古 1:5 万高力罕牧场三连等四幅区域地质矿产调查中,新识别和填绘出呼都格奥长花岗岩体。1:20 万罕乌拉幅区域地质调查将该岩体划归为华力西晚期石英闪长岩,1:25 万西乌珠穆沁旗幅区域地质调查将其归为二叠纪石英闪长岩,均缺少地球化学和年代学等资料。因此,本文在 1:5 万区域地质调查的基础上,选择贺根山缝合带梅劳特乌拉蛇绿岩北侧呼都格岩体(图 1,2)进行岩石学、锆石年代学和地球化学研究,讨论岩石成因、构造环境和形成时代,并结合梅劳特乌拉-高力罕蛇绿岩-TTG 岩带中的前弧玄武岩、高镁安山岩/高镁闪长岩-镁安山岩、埃达克岩、TTG、富铌弧玄武岩/辉长岩等岛弧火成岩的共生组合关系,探讨 TTG 岩浆事件与二连-贺根山洋盆俯冲消亡时间与过程,以期能够为古亚洲洋俯冲消亡过程与新生陆壳生长构造岩浆事件提供约束。

1 区域地质背景和岩石学特征

内蒙古西乌珠穆沁旗高力罕地区呼都格岩体,位于二连-贺根山缝合带东段梅劳特乌拉-高力罕北东向蛇绿岩-TTG 岩带内(图 1,2),大地构造位置属于华北板块北缘增生带与西伯利亚板块南缘增生带缝合区。呼都格岩体出露于梅劳特乌拉蛇绿岩北侧(图 1,图 2)(Li Yingjie et al., 2015; Wang Jinfang et al., 2017a, 2017b, 2018a, 2018b, 2019a, 2019b),侵入于高力罕地区晚石炭世早期奥长花岗岩(315.76 ± 0.94 Ma)之中,被晚石炭世晚期英云闪长岩(305.6 ± 1.5 Ma)所侵入,晚侏罗世(158.98 ± 0.72 Ma)满克头鄂博组火山岩覆盖其上,出露面积

约 54 km^2 (图 2)。呼都格岩体边部为细粒奥长花岗岩,中部为粗中粒奥长花岗岩,粗中粒奥长花岗岩侵入于细粒奥长花岗岩之中。岩石呈灰白色和浅灰色,细粒-粗中粒半自形粒状结构,块状构造(图 3),矿物成分主要为斜长石(55%~65%)、石英(30%~35%)和黑云母(3%~4%),少量钾长石(±2%)等。斜长石多呈半自形短柱状和板状,发育聚片双晶,双晶纹细密,近于平行消光,根据垂直{010}最大消光角法测得 $\text{An}=22$,属于更长石,部分颗粒强烈高岭土化和绢云母化。石英他形粒状。黑云母为自形片状,可见绿泥石化。

2 样品采集与分析测试方法

2.1 锆石 U-Pb 测年

本文在呼都格岩体中采集了 2 件新鲜的锆石年龄样品(P1608 和 P2704),采样地理位置分别为 $N45^{\circ}03'16''$ 、 $E118^{\circ}27'41''$ 和 $N45^{\circ}01'34''$ 、 $E118^{\circ}18'32''$ (图 2)。样品 P1608 和 P2704 锆石的挑选工作由河北省区域地质矿产调查研究所实验室完成。首先,将岩石样品破碎成粉末;第二步,运用重液和磁选法分离技术进行锆石的分选;第三步,在双目镜下挑选出晶形相对完好、无色透明、无包裹体和裂纹的测试锆石;第四步,用环氧树脂在玻璃板上固定挑选好的锆石与标样抛光至锆石中心制靶;第五步,利用双目镜和阴极发光(CL)图像研究样品锆石的晶形和内部结构,选择原位同位素分析的最佳点。本文样品锆石制靶和阴极发光实验在北京锆年领航科技有限公司完成。LA-ICP-MS 锆石 U-Pb 年龄测试工作由天津地质调查中心完成,使用仪器为 Neptune 多接收电感耦合等离子体质谱仪和 193 nm 激光取样系统(LA-MC-ICP-MS),激光剥蚀斑束直径为 $35\mu\text{m}$,激光剥蚀样品的深度为 $20\sim40\mu\text{m}$ 。最后,完成锆石样品测试数据的普通铅校正处理、U-Pb 年龄谐和图绘制和年龄权重平均计算工作(Ludwig, 2003)。

2.2 岩石地球化学测试分析

本次研究工作在西乌旗呼都格岩体中采集了 10 件新鲜的岩石地球化学样品,主量和微量元素分析由河北省廊坊区域地质矿产研究所完成。首先,将岩石样品在破碎机上进行粗碎;然后,在玛瑙钵体和柱头研磨机上研磨至 200 目以下;最后,主量元素分析采用 Axios^{max}X 射线荧光光谱仪测定,精度在 1% 以内;微量元素和稀土元素采用 X-Series 2 等离子体质谱仪测定,测试精度在 5% 以内。

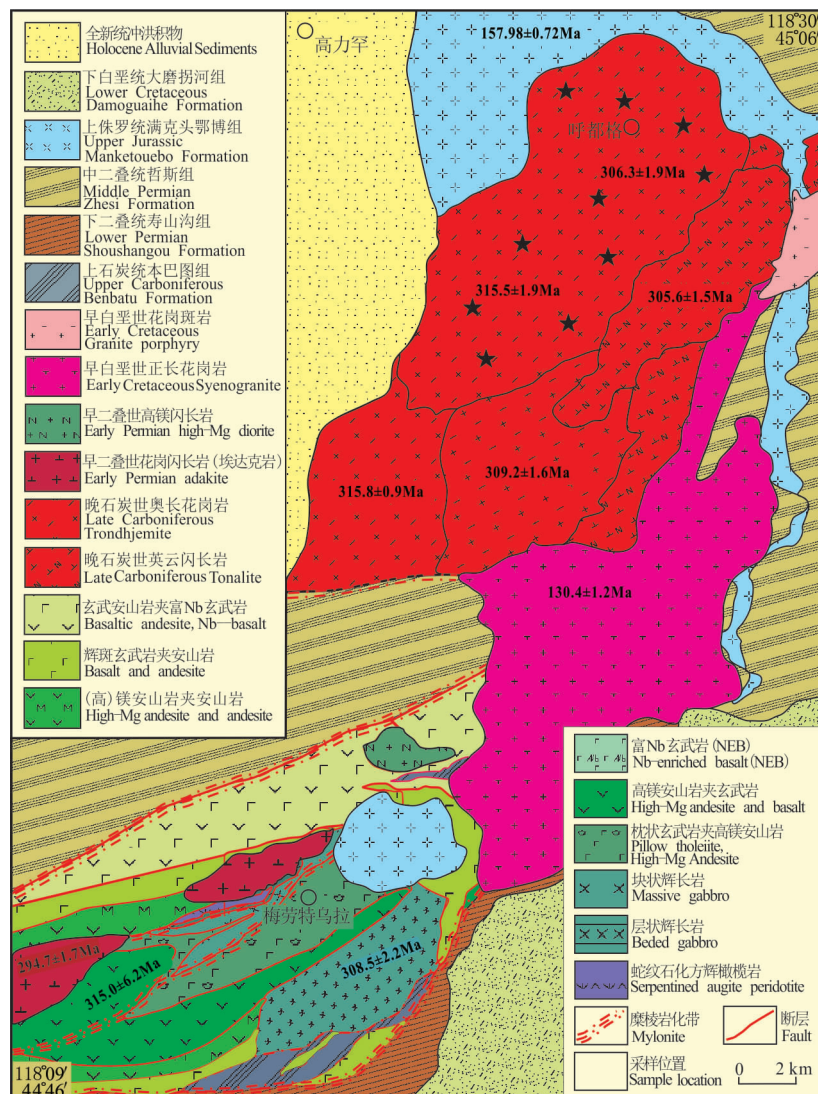


图2 梅劳特乌拉-高力罕蛇绿岩-TTG 岩带呼都格奥长花岗岩地质简图

Fig. 2 Sketch geological map of the Hudege trondhjemite in the Meilaotewula-Gaolian ophiolite-TTG belt

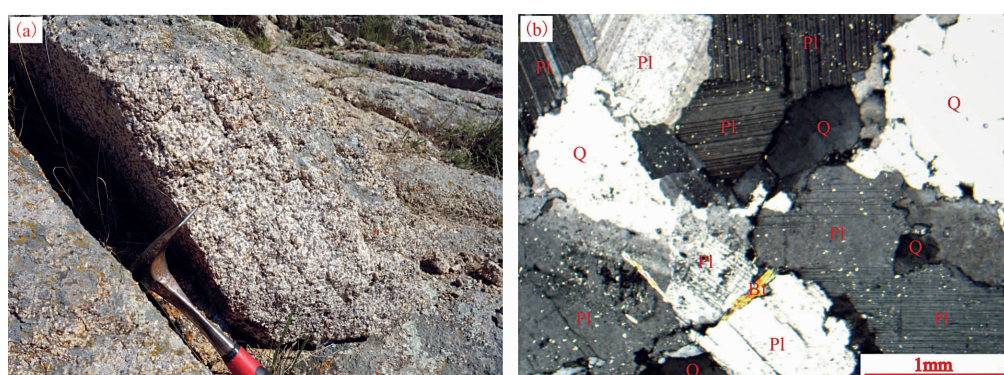


图3 呼都格奥长花岗岩野外(a)和显微照片(b)

Fig. 3 Representative field photos (a) and photomicrograph (b) of the Hudege trondhjemite

Pl—斜长石; Q—石英; Bt—黑云母

Pl—Plagioclase; Q—quartz; Bt—biotite

3 分析结果

3.1 长石 U-Pb 年代学

长石 U-Pb 测试结果如图 4、图 5 和表 1。如图 4 所示,呼都格岩体 P1608 样品(28 粒长石)和 P2704 样品(25 粒长石)的阴极发光图像(CL)显示其结构均一,自形程度较高,为晶形完好的自形—半自形柱状和双锥状,长宽比为 1:1~3:1,具有清晰的晶棱、晶面、振荡环带和明暗相间的条带结构,岩浆结晶环带相对较窄而且自形生长环带较为清晰密集,外部无变质边,内部无残留核(图 4),显示酸性岩浆成因长石特征。

如表 1 所示,除 P1608 样品的 19 号点和 P2704 样品的 1 号、20 号点之外,呼都格岩体两组样品的 27 粒、23 粒长石测定的 Th/U 比值均大于 0.1,分

别在 0.3149~0.7524 和 0.1392~0.7187 之间,显示测试样品长石为酸性岩浆成因(Corfu et al., 2003; Wu Yuanbao et al., 2004)。

LA-ICP-MS 长石 U-Pb 定年结果显示(表 1, 图 4, 图 5),P1608 和 P2704 样品长石的测点位于震荡环带发育部位,测定的数据点集中于谐和线上及其附近,分别获得 $^{206}\text{Pb}/^{238}\text{U}$ 年龄加权平均值为 306.3 ± 1.9 Ma (MSWD = 2.5) 和 315.5 ± 1.9 Ma (MSWD = 2.7),代表了该岩体的侵位结晶年龄(表 1, 图 5),表明西乌旗呼都格岩体的形成时代为晚石炭世。

3.2 主量元素

如表 2 所示,呼都格岩体总体表现出高硅富铝和富钠贫钾的主量元素特征。其中, SiO_2 含量介于 66.27%~71.59% 之间,平均值 69.44%; Al_2O_3 含

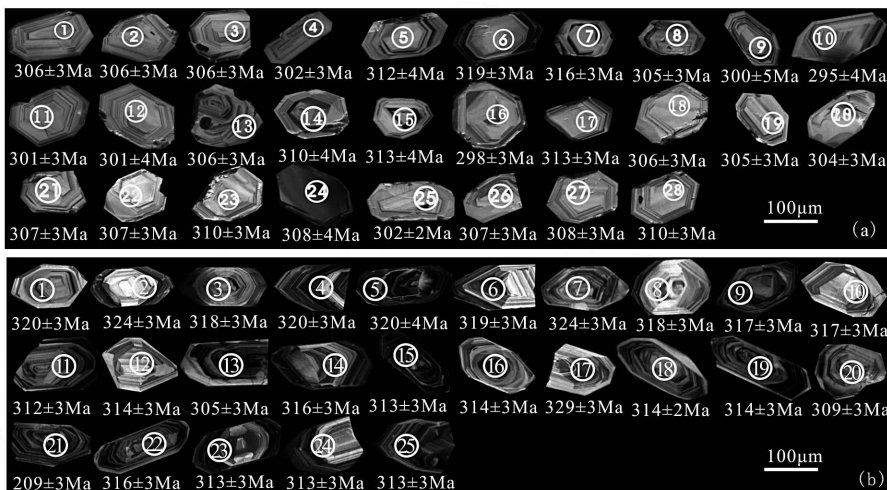


图 4 呼都格岩体 P1608 (a) 和 P2704 (b) 样品长石阴极发光图像及其 LA-ICP-MS U-Pb 年龄

Fig. 4 Zircon cathodoluminescent images and LA-ICP-MS U-Pb ages of sample P1608 (a) and P2704 (b) from the Huduge trondhjemite

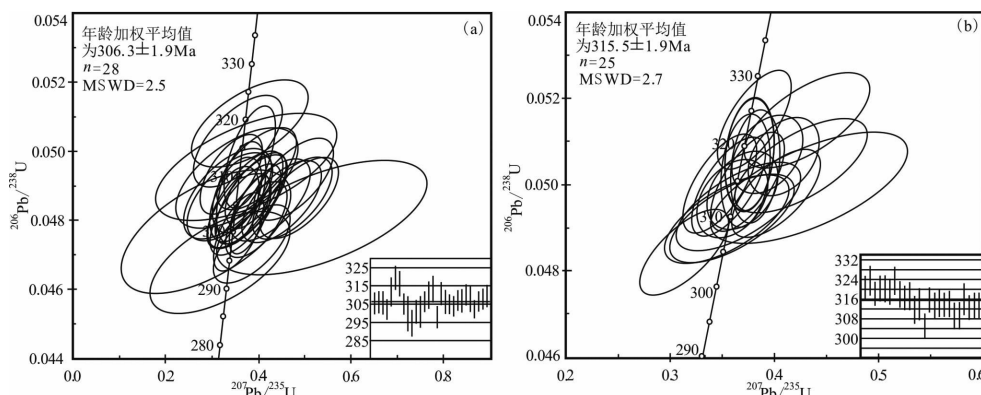


图 5 呼都格岩体 P1608 (a) 和 P2704 (b) 样品长石 LA-ICP-MS U-Pb 年龄谐和图和直方图

Fig. 5 Zircon U-Pb concordia diagram and histograms of sample P1608 (a) and P2704 (b) from the Huduge trondhjemite

表 2 呼都格岩体主量(%)、微量($\times 10^{-6}$)和稀土元素($\times 10^{-6}$)分析结果Table 2 Major element (%), trace element ($\times 10^{-6}$) and REE ($\times 10^{-6}$) analyses of the Huduge trondhjemite

样号	P1604	P1605	P1606	P1607	P1608	P1609	P2702	P2703	P2704	P2705	显生宙 TTG	高 Si 埃达克岩
SiO ₂	66.27	67.79	70.44	70.91	68.36	69.10	71.59	70.32	70.67	68.98	65.9	64.8
TiO ₂	0.54	0.50	0.34	0.28	0.45	0.44	0.20	0.31	0.28	0.36	0.47	0.56
Al ₂ O ₃	15.94	15.48	15.26	15.23	15.60	15.57	15.27	15.72	15.17	15.51	16.5	16.64
Fe ₂ O ₃	2.21	1.79	1.48	1.15	1.76	0.86	1.18	1.25	1.69	1.96	4.11	4.75
FeO	1.53	1.41	1.03	0.84	1.39	1.84	0.42	0.96	0.84	1.25		
MnO	0.07	0.06	0.06	0.05	0.07	0.06	0.048	0.052	0.054	0.063	0.09	0.081
MgO	1.53	1.52	0.87	0.75	1.32	1.38	0.57	0.89	0.92	1.23	1.67	2.18
CaO	3.67	2.97	1.60	1.95	2.80	1.48	0.78	0.81	1.14	2.18	4.36	4.63
Na ₂ O	4.49	4.13	4.92	4.74	4.71	4.90	6.59	5.96	5.43	4.99	4	4.19
K ₂ O	1.88	2.47	2.34	2.53	2.03	2.27	1.79	1.89	1.96	1.72	2.14	1.97
P ₂ O ₅	0.15	0.13	0.11	0.09	0.14	0.13	0.08	0.11	0.11	0.14	0.12	0.2
LOI	1.58	1.62	1.42	1.35	1.25	1.88	1.39	1.57	1.49	1.51		
Total	99.86	99.87	99.88	99.87	99.88	99.91	99.91	99.83	99.76	99.89		
Mg [#]	44	47	40	42	44	48	41	43	41	42	45	48
La	13.40	14.42	12.46	10.33	12.90	17.12	8.56	9.96	10.05	10.03	17	19.2
Ce	30.93	33.45	27.06	22.78	30.05	32.88	16.03	21.13	19.50	20.69	34	37.3
Pr	4.12	4.45	3.24	3.00	4.02	4.25	1.89	2.65	2.45	2.74		
Nd	16.78	17.75	12.44	11.84	16.15	17.51	7.36	10.35	9.98	11.12	16	18.2
Sm	3.28	3.44	2.45	2.21	3.11	3.34	1.46	1.95	2.01	2.23	3.1	3.4
Eu	0.99	0.97	0.71	0.63	0.90	1.03	0.47	0.59	0.64	0.74	0.84	0.9
Gd	2.74	2.80	1.96	1.80	2.56	2.76	1.23	1.65	1.63	1.84	2.8	2.8
Tb	0.43	0.44	0.31	0.27	0.40	0.41	0.20	0.27	0.25	0.29	0.4	
Dy	2.52	2.57	1.80	1.61	2.28	2.30	1.17	1.56	1.44	1.67		1.9
Ho	0.47	0.48	0.33	0.30	0.42	0.42	0.20	0.27	0.26	0.31		
Er	1.33	1.40	0.98	0.91	1.26	1.24	0.59	0.81	0.78	0.91		0.96
Tm	0.22	0.24	0.17	0.16	0.22	0.20	0.09	0.13	0.12	0.15		
Yb	1.41	1.52	1.04	1.06	1.36	1.21	0.59	0.79	0.81	0.92	1.16	0.88
Lu	0.20	0.22	0.17	0.16	0.20	0.19	0.11	0.12	0.11	0.13	0.18	0.17
Σ REE	78.83	84.14	65.10	57.04	75.82	84.87	39.95	52.23	50.03	53.77		
Y	12.00	12.63	8.67	8.16	11.40	11.21	5.7	7.51	7.12	8.14	14.5	10
Ba	444.70	480.60	464.40	472.20	383.60	395.10	338.10	408.10	368.20	348.20	716	721
Rb	28.70	39.81	40.65	41.12	35.22	28.75	24.94	23.32	25.94	23.51	63	52
Sr	465.40	384.60	384.00	377.90	391.60	306.20	196.60	307.70	232.40	369.50	493	565
Zr	101.09	97.19	93.97	88.10	94.60	95.36	76.75	82.92	87.45	92.57	122	108
Nb	3.62	3.98	3.24	2.77	3.02	2.66	1.99	1.89	1.81	2.08	6.7	6
Th	3.70	5.26	5.66	4.96	3.44	4.23	1.58	1.55	2.46	3.02	7.6	
Ni	4.64	4.15	3.54	2.83	3.57	4.82	3.41	3.93	4.76	6.92	12	20
V	77.22	64.01	50.07	38.98	60.58	66.68	25.93	36.51	44.16	61.27		95
Cr	9.66	7.26	5.96	5.33	6.48	7.78	4.23	4.95	6.17	7.85	32	41
Hf	8.70	9.63	4.77	6.48	8.23	8.88	4.13	5.25	6.57	6.79	3.4	
Sc	6.89	6.32	4.93	4.83	5.67	5.89	4.32	4.79	5.93	6.62		
Ta	0.34	0.36	0.33	0.24	0.30	0.23	0.15	0.17	0.18	0.20	0.75	
Co	9.11	7.50	5.53	3.86	6.71	7.72	3.52	4.76	5.57	7.15		
Li	18.86	19.62	20.53	12.44	20.13	14.62	7.65	12.14	12.50	16.48		
U	1.05	1.44	0.74	1.15	0.74	0.76	0.43	0.32	0.52	0.62	1.9	

注:高 Si 埃达克岩为 267 个样品平均值(Martin et al., 2005),显生宙 TTG 为 698 个样品平均值(Condie, 2005)。

量为 15.23%~15.94%, 平均值 15.48%; Na₂O 含量为 4.13%~6.59%, 平均值 5.09%; K₂O 含量为 1.72%~2.53%, 平均值 2.09%; Na₂O/K₂O 比值为 1.67~3.68, 平均值 2.50; 全碱(Na₂O+K₂O)含量为 6.37%~8.38%, 平均值 7.17%。岩石的里特曼指数 σ 为 1.71~2.44, 平均值 1.93, 为钙碱性岩。

岩石的 MgO 含量为 0.57%~1.53%, 平均值 1.10%, Mg[#] 40~48, 平均值 43, 相对较低; 相对贫 TiO₂(0.20%~0.54%) 和 P₂O₅(0.08%~0.15%)。

呼都格岩体的铝饱和指数 A/CNK 值介于 0.99~1.18 之间, A/NK 为 1.20~1.69, 属准铝质-强过铝质。在 SiO₂-K₂O 图(图 6)中, 所有 10 个样

品均投在中钾钙碱性系列范围内,指示其为中钾钙碱性系列岩石。在 $\text{SiO}_2-(\text{Na}_2\text{O}+\text{K}_2\text{O})$ (TAS)分类图解中,呼都格岩体样品投在亚碱性花岗闪长岩与花岗岩的过渡区域(图 7)。在 An-Ab-Or 图解中,该岩石有 7 个样品落在奥长花岗岩区,1 个样品落在奥长花岗岩与英云闪长岩的交界处,另有 2 个样品分别落入英云闪长岩区和花岗岩闪长岩区(图 8)。在 K-Na-Ca 图解(图 9)中,呼都格岩体所有 10 个样品均落在太古宙 TTG 区域,样品投点呈现出奥长花岗岩演化趋势。

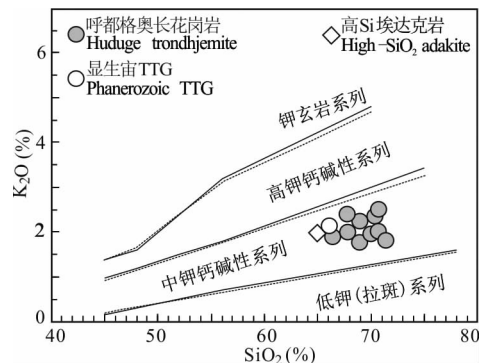


图 6 呼都格岩体 $\text{SiO}_2-\text{K}_2\text{O}$ 分类图解

(据 Peccerillo et al., 1976)

Fig. 6 $\text{SiO}_2-\text{K}_2\text{O}$ classification diagrams of the Huduge trondhjemite (after Peccerillo et al., 1976)

3.3 稀土元素

在稀土元素特征上(表 2),呼都格岩体的稀土元素含量相对较低, ΣREE 为 $39.95 \times 10^{-6} \sim 84.87 \times 10^{-6}$,平均值 64.18×10^{-6} ;Yb 和 Y 含量明显较低,分别为 $0.59 \times 10^{-6} \sim 1.52 \times 10^{-6}$ (平均值 1.07×10^{-6})和 $5.70 \times 10^{-6} \sim 12.63 \times 10^{-6}$ (平均值 9.25×10^{-6})。呼都格岩体的 δEu 为 $0.93 \sim 1.09$,平均值 0.99,铕异常不明显;(La/Yb)_N变化范围为 $6.39 \sim 9.78$,轻重稀土分离明显,球粒陨石标准化的稀土元素配分曲线为右倾模式(图 10)。

3.4 微量元素

如表 2 所示,呼都格岩体的 Sr 含量和 Sr/Y 比值相对较高,分别为 $196.60 \times 10^{-6} \sim 465.40 \times 10^{-6}$ (平均值 341.59×10^{-6})和 $27.31 \sim 46.31$ (平均值 37.50);岩石的 Ni 和 Cr 含量相对较低,分别为 $2.83 \times 10^{-6} \sim 6.92 \times 10^{-6}$ (平均值 4.26×10^{-6})和 $4.23 \times 10^{-6} \sim 9.66 \times 10^{-6}$ (平均值 6.57×10^{-6})。在原始地幔标准化的微量元素比值蛛网图中(图 11),呼都格岩体呈现出明显的 Sr 等正异常和 Nb、Ta、Ti、P 负异常,可能反映了大洋俯冲带岛弧型

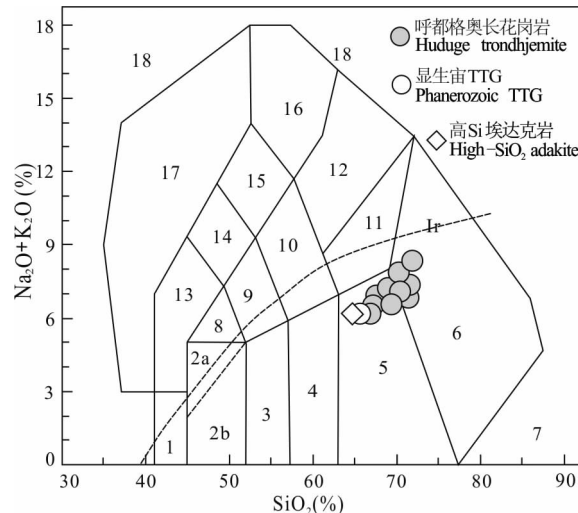


图 7 呼都格岩体 TAS 分类图(据 Middlemost, 1994)

Fig. 7 Total alkalis vs. silica (TAS) classification diagram of the Huduge trondhjemite (after Middlemost, 1994)

1—橄榄辉长岩;2a—碱性辉长岩;2b—亚碱性辉长岩;3—辉长闪长岩;4—闪长岩;5—花岗闪长岩;6—花岗岩;7—硅英岩;8—二长辉长岩;9—二长闪长岩;10—二长岩;11—石英二长岩;12—正长岩;13—副长石辉长岩;14—副长石二长闪长岩;15—副长石二长正长岩;16—副长正长岩;17—副长深成岩;18—霓方钠岩/磷霞岩/粗白榴岩

1—Olivine gabbro; 2a—alkaline gabbro; 2b—subalkaline gabbro; 3—gabbro diorite; 4—diorite; 5—granodiorite; 6—granite; 7—silicalite; 8—monzogabbro; 9—monzodiorite; 10—monzonite; 11—quartz monzonite; 12—syenite; 13—parafeldspar gabbro; 14—parafeldspar monzodiorite; 15—parafeldspar monzosyenite; 16—parafeldspar syenite; 17—parafeldspar pluton; 18—aegirine sodalite/nepheline/leucite

TTG 侵入岩的微量元素组分特征与岩浆源区性质。

4 讨论

4.1 岩石属性、成因与构造环境

呼都格岩体富钠 (Na_2O 平均值 5.09%)、富硅 (SiO_2 平均值 $69.44\% > 56\%$)、高铝 (Al_2O_3 平均值 $15.48\% > 15\%$)、高 $\text{Na}_2\text{O}/\text{K}_2\text{O}$ (平均值 $2.50 > 2$)、高锶 (Sr 平均值 341.59×10^{-6})、高 Sr/Y (平均值 $37.50 \approx 40$),低镁 (MgO 平均值 $1.10\% < 3\%$)、低镱 (Yb 平均值 $1.07 \times 10^{-6} < 1.9 \times 10^{-6}$),低钇 (Y 平均值 $9.25 \times 10^{-6} < 18 \times 10^{-6}$),与显生宙 TTG 和高 Si 埃达克岩相类似(表 2,图 6~9)。该岩体富集轻稀土、亏损重稀土,无明显的 Eu 异常,与显生宙 TTG 和高 Si 埃达克岩的稀土配分曲线分布形式基本一致(图 10)。岩石相对富集大离子亲石元素 Ba、K、Rb、Sr 等,相对亏损高场强元素 Nb、Ta、P、Ti 等,其微量元素原始地幔标准化蛛网图分布曲线与

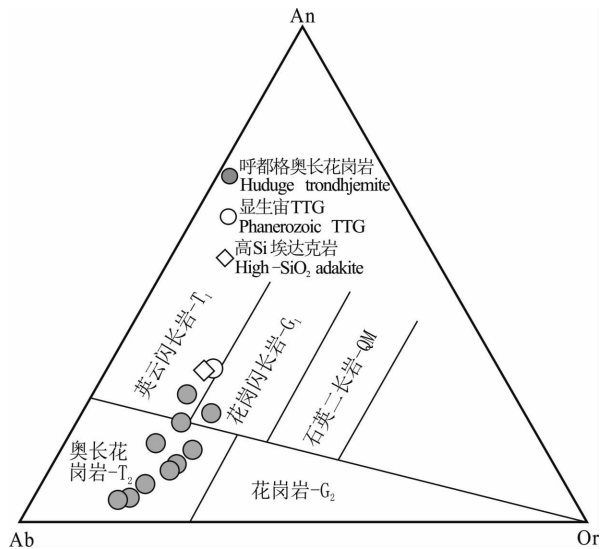


图 8 呼都格岩体 An-Ab-Or 分类图解(据 O'Connor, 1965)

Fig. 8 An-Ab-Or classification diagram of the Huduge trondhjemite (after O'Connor, 1965)

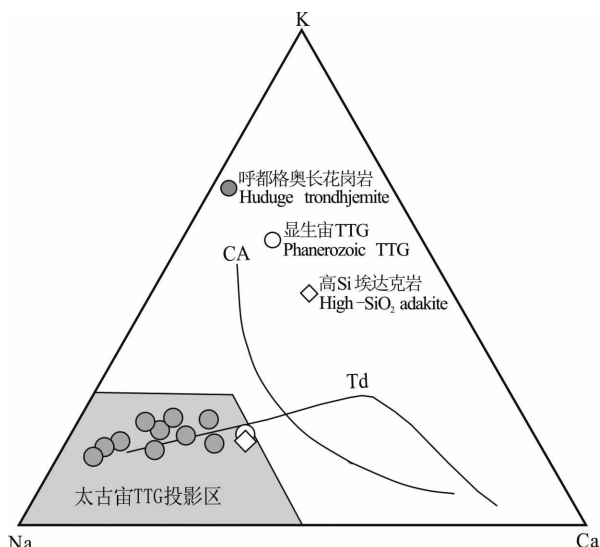


图 9 呼都格岩体 K-Na-Ca 图解(据 Martin et al., 2005)

Fig. 9 K-Na-Ca diagram of the Huduge trondhjemite
(after Martin et al., 2005)

CA—岛弧区钙碱性岩浆演化趋势；Td—奥长花岗质岩浆演化趋势
CA—Classical calc-alkaline trend；Td—trondhjemitic
differentiation trend

显生宙 TTG 和高 Si 埃达克岩相吻合(图 11)。但是,呼都岩体与高 Si 埃达克岩相类比, SiO_2 含量更高,而 Mg 含量和 $Mg^{\#}$ 值相对偏低,Sr 和 Cr、Ni 含量也相对较低。而且,呼都格岩体呈现出奥长花岗质岩浆演化趋势(图 9),具有典型的 $T_1 T_2 G_1$ 组合演化趋势特征(图 8)。因此,通过岩石学特征和主量、稀土、微量元素与显生宙 TTG 和高 Si 埃达克岩的对比(表 2,图 6~7),并参考 An-Ab-Or 分类图解

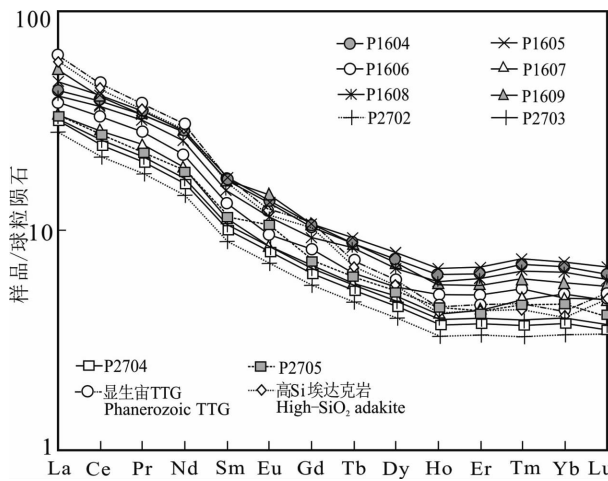


图 10 呼都格岩体稀土元素球粒陨石标准化配分模式
(据 Sun et al., 1989)

Fig. 10 Chondrite-normalized REE distribution patterns
of the Huduge trondhjemite (after Sun et al., 1989)

(图 8)、K-Na-Ca 图解(图 9)、稀土元素配分图(图 10)和微量元素蛛网图等(图 11),呼都格岩体应归属属于高铝 TTG 岩类的 $T_1 T_2 G_1$ 组合(Martin et al., 2005; Condie, 2005; Feng Yanfang et al., 2011; Zhang Qi et al., 2012; Wu Mingqian et al., 2014; Deng Jinfu et al., 2015a, 2018)。

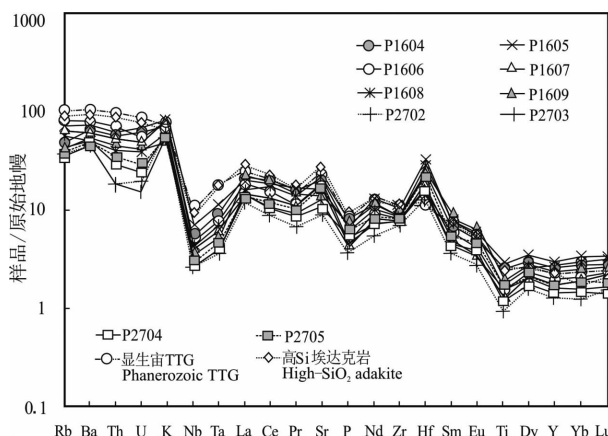


图 11 呼都格岩体微量元素原始地幔标准化蛛网图
(据 Sun et al., 1989)

Fig. 11 Primitive mantle-normalized trace element spider diagram of the Huduge trondhjemite (after Sun et al., 1989)

对于 TTG 的成因,地球化学和高温高压实验岩石学研究已证明其形成于含水玄武质岩石在石榴角闪岩相或榴辉岩相的部分熔融(Condie, 1986; Martin, 1987; Rapp et al., 1991, 1995; Foley et al., 2002; Xiong, 2006)。但是对于 TTG 的成因方式或形成的构造环境,还存在着主要两种不同的观点与

争议。①俯冲洋壳(板片)玄武岩脱水部分熔融成因,认为显生宙 TTG 与大洋俯冲成因的高 Si 埃达克岩(O型)类似,并与前弧玄武岩、玻安岩(高镁安山岩/高镁闪长岩)和富铌玄武岩/富铌辉长岩成因有关,主要为(大洋)岛弧地区大洋俯冲板片玄武岩部分熔融的产物(Defant et al., 1990; Rapp et al., 1991, 1995; Yogodzinski et al., 1995; Martin, 1999; Foley et al., 2002; Martin et al., 2005; Jiang Yang et al., 2014; Deng Jinfu et al., 2015a, 2018)。②加厚镁铁质下地壳的部分熔融成因,认为 TTG 岩类与大洋俯冲无关,是加厚镁铁质下地壳部分熔融的产物,类似于加厚镁铁质下地壳部分熔融形成的埃达克岩(C型)(Condie, 2005; Smithies et al., 2009; Liu Jianhui et al., 2015)。但是,对于显生宙 TTG 的成因,大洋俯冲玄武岩板片脱水熔融成因的认识被广泛接受(Rapp et al., 1995; Drummond et al., 1996; Foley et al., 2002; Feng Yanfang et al., 2011; Wu Mingqian et al., 2014; Deng Jinfu et al., 2015a, 2018)。

呼都格 $T_1 T_2 G_1$ 组合具明显的大洋俯冲带岛弧岩浆岩的地球化学特征,并与南侧的梅劳特乌拉晚石炭世(—早二叠世)蛇绿岩中的前弧玄武岩(枕状拉斑玄武岩)、玻安岩(高镁安山岩/高镁闪长岩)-镁安山岩、高 Si 埃达克岩(花岗闪长岩和英云闪长岩或 TTG)、富铌玄武岩/富铌辉长岩等构成较为完整的(洋内)弧火成岩构造组合(图 1,2)(Li Yingjie et al., 2015; Wang Jinfang et al., 2017a, 2017c, 2018a, 2018b, 2019a, 2020a, 2020b),表明呼都格 $T_1 T_2 G_1$ 组合可能源自大洋岛弧区洋内大洋俯冲板片玄武岩的部分熔融。而且,呼都格 $T_1 T_2 G_1$ 为中钾钙碱性系列(图 6),具有明显较高的 Na_2O 和 Al_2O_3 含量(表 2),属高铝 TTG。与显生宙高钾壳源花岗岩大多为钙碱性岩浆演化趋势(CA)明显不同(图 9),呼都格 $T_1 T_2 G_1$ 属于富钠的单独的花岗岩浆系列, Na_2O/K_2O 平均值 $2.50\% > 2\%$,在 K-Na-Ca 三角图中为奥长花岗质岩浆演化趋势(Td),呈现出向富钠方向演变特征(图 9)(Defant et al., 1990; Stern et al., 1996; Samaniego et al., 2002; Bourdon et al., 2003; Martin et al., 2005; Deng Jinfu et al., 2015a)。但是,也应当指出,该岩体两件锆石 U-Pb 年龄的差异($306.3 \pm 1.9\text{ Ma}$, $315.5 \pm 1.9\text{ Ma}$)和一些样品 CaO 等含量的较大变化(P2702 和 P2703 的 CaO 含量明显较低,而 P1604 和 P1605 的 CaO 含量明显较高),是否又反映还存

在两个期次岩浆活动的可能,尚需进一步讨论。

在 $Yb_N-(La/Yb)_N$ 部分熔融图解上(图 12),呼都格 $T_1 T_2 G_1$ 主要分布在石榴石-斜长角闪岩为残留相的高铝 TTG 区域内,表明呼都格 $T_1 T_2 G_1$ 起源于玄武岩在石榴石和角闪石等为主要残留相的部分熔融,反映该 $T_1 T_2 G_1$ 可能为洋壳玄武质的低钾玄武岩类在较高温度下较高程度部分熔融成因。在 SiO_2-MgO 和 $(CaO+NaO_2)-Sr$ 图解中(图 13),呼都格 $T_1 T_2 G_1$ 10 个样品均落入玄武岩熔融熔体范围内,并与显生宙 TTG 平均值投点吻合。这些地球化学图解表明该 $T_1 T_2 G_1$ 的物质来源或源区与洋壳玄武岩部分熔融物质的亲缘性,表明该 $T_1 T_2 G_1$ 为大洋俯冲玄武岩板片脱水部分熔融成因,属于形成于大洋俯冲带岛弧环境的特殊的岛弧型富钠岩浆岩(Beard, 1991; Defant, 1993; Rapp et al., 1999; Foley et al., 2003; Martin et al., 2005; Deng Jinfu et al., 2015a)。而且,呼都格岩体的源区特征与南部邻区西乌旗迪彦庙-达青俯冲增生杂岩内晚石炭世大洋斜长花岗岩锆石 Hf 同位素高的($^{176}\text{Hf}/^{177}\text{Hf}_t$)比值($0.28294 \sim 0.28300$)和正的 $\epsilon_{\text{Hf}}(t)$ 值($12.878 \sim 14.215$)所揭示的地幔源区相吻合(Cheng Yang et al., 2020),与西部邻区贺根山-崇根山蛇绿岩内早石炭世洋内初始俯冲形成的前弧玄武岩相对应(Wang Cheng et al., 2019),为呼都格岩体的洋内弧环境判别提供了进一步的证据。

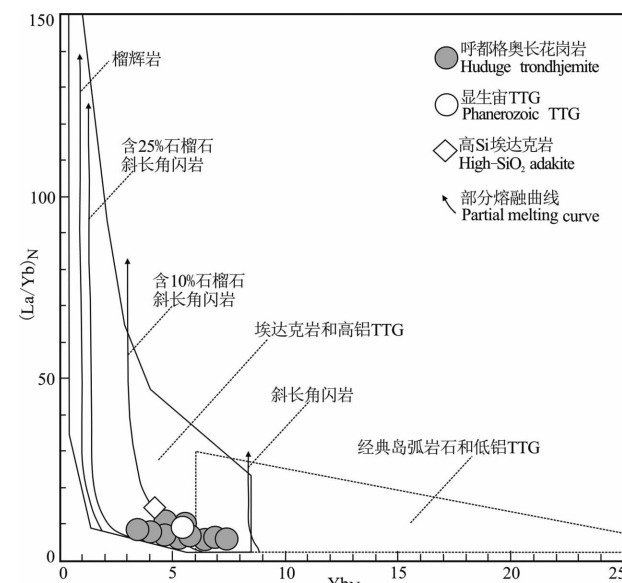
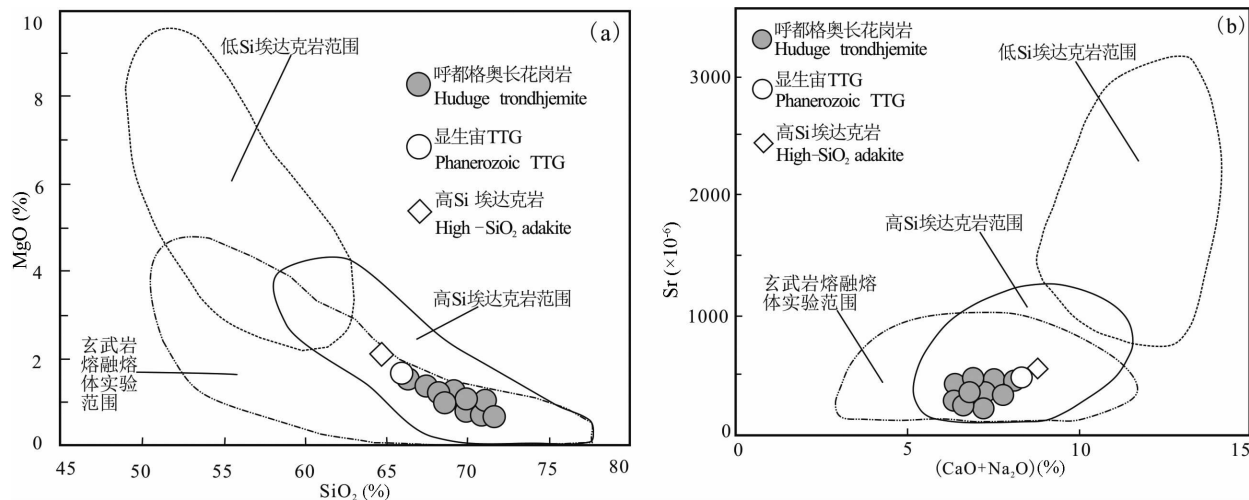


图 12 呼都格岩体 $Yb_N-(La/Yb)_N$ 构造判别图解

(据 Defant et al., 1990; Martin, 1999)

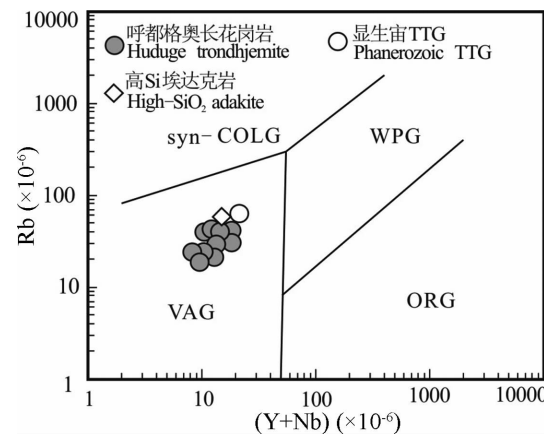
Fig. 12 $Yb_N-(La/Yb)_N$ tectonic discriminant diagrams of the Huduge trondhjemite(after Defant et al., 1990; Martin, 1999)

图 13 呼都格岩体 $\text{SiO}_2\text{-MgO}$ (a) 和 $(\text{CaO}+\text{Na}_2\text{O})\text{-Sr}$ (b) 图解(据 Martin et al., 2005)Fig. 13 $\text{SiO}_2\text{-MgO}$ (a) and $(\text{CaO}+\text{Na}_2\text{O})\text{-Sr}$ (b) diagrams of the Huduge trondhjemite (after Martin et al., 2005)

在 Rb-(Y+Nb) 构造环境判别图解上(图 14),呼都格 $T_1 T_2 G_1$ 10 个样品均投在火山岛弧区域,而且其投点区域与显生宙 TTG 平均值投点区域相重叠,表明其形成于岛弧环境(Thorkelson et al., 2005; Viruete et al., 2007; Deng Jinfu et al., 2015a)。在 $\text{Yb}_{\text{N}}\text{-(La/Yb)}_{\text{N}}$ 图解中(图 12),呼都格 $T_1 T_2 G_1$ 有 7 个样品投在岛弧型高铝 TTG 区域,3 个样品投在高铝 TTG 与低铝 TTG 的重叠区域,全部 10 个样品其投点区域与显生宙 TTG 平均值投点相重叠,表明其形成于大洋俯冲 TTG 岩浆岛弧环境(Deng Jinfu et al., 2015a; Xue Jianping et al., 2018; Wang Shuqing et al., 2018)。

4.2 形成时代与 TTG 岩浆事件

近十几年来,中亚造山带东段二连-贺根山缝合带区域内获得大量石炭纪一二叠纪蛇绿岩和岛弧型岩浆岩的形成时代数据。通过锆石 U-Pb 年代学和放射虫硅质岩生物地层学研究,在二连-贺根山缝合带区域内获得了许多早石炭世—晚石炭世蛇绿岩年龄数据(Jian Ping et al., 2012; Li Yingjie et al., 2015, 2018b, 2018c),以及早二叠世(—中二叠世早期)蛇绿岩年代证据(Wang Hui et al., 2005; Li Gangzhu et al., 2017)。而对应于石炭纪—早、中二叠世蛇绿岩的时空分布,二连-贺根山缝合带区域内还获得了大量早石炭世—晚石炭世岛弧岩浆岩(Chen Bin et al., 2009; Liu Jianfeng et al., 2009, 2013; Kang Jianli et al., 2016; Wang Shuqing et al., 2018; Wang Jinfang et al., 2019a, 2020a, 2020b)和早、中二叠世岛弧岩浆岩(Jian Ping et al., 2010; Wang Jinfang et al., 2017a, 2017c,

图 14 呼都格岩体 Rb-(Y+Nb) 构造判别图解

(据 Pearce et al., 1984)

Fig. 14 Rb-(Y+Nb) tectonic discriminant diagrams of the Huduge trondhjemite (after Pearce et al., 1984)
syn-COLG—同碰撞花岗岩; VAG—火山弧花岗岩; WPG—板内花岗岩; ORG—洋脊花岗岩

syn-COLG—Syn-collision granites; VAG—volcanic arc granites;
WPG—within plate granites; ORG—ocean ridge granites

2018a, 2018b; Xue Jianping et al., 2018; Cheng Yang et al., 2019)的锆石 U-Pb 年龄数据。在这些早石炭世—中二叠世岛弧岩浆岩中,地质工作者不断识别和揭露岛弧岩浆岩组合(Chen Bin et al., 2000; Xue Jianping et al., 2018; Wang Shuqing et al., 2018; Wang Jinfang et al., 2019a)。这些 TTG 岩石组合的锆石 U-Pb 年龄分布在早石炭世末—早二叠世末的 330~266 Ma 之间,但明显集中分布在 320~295 Ma 的晚石炭世,特别是西乌旗梅劳特乌拉蛇绿岩-TTG 岩带内的 TTG 岩石组合明显集中

分布在晚石炭世,指示晚石炭世的重要 TTG 岩浆事件与新生陆壳增生作用(Wang Shuqing et al., 2018; Wang Jinfang et al., 2019a) (本文及未发表数据,图 2)。这些 TTG 岩石组合为二连-贺根山缝合带区域内已知最主要的晚石炭世岩石之一,代表了晚石炭世的重要岩浆活动与陆壳增生作用。

本文研究的高力罕地区呼都格岩体 $T_1 T_2 G_1$ 岩石组合,是梅劳特乌拉-高力罕蛇绿岩-TTG 岩带的重要组成部分(图 1,2),其侵入于晚石炭世早期奥长花岗岩(TTG)(315.76 ± 0.94 Ma)之中,被晚石炭世晚期英云闪长岩(TTG)(305.6 ± 1.5 Ma)所侵入(图 2)。通过 LA-ICP-MS 锆石 U-Pb 定年,本次研究工作在呼都格岩体中获得了 306.3 ± 1.9 Ma 和 315.5 ± 1.9 Ma 两组年龄,表明其形成于晚石炭世。呼都格岩体的形成时代与高力罕晚石炭世 TTG 岩带(岩浆弧)和南侧梅劳特乌拉晚石炭世(—早二叠世)蛇绿岩(-洋内弧火成岩)以及二连-贺根山缝合带区域内石炭纪一二叠纪蛇绿岩、岛弧型岩浆岩的形成时代相吻合(Miao Laicheng et al., 2008; Liu Jianfeng et al., 2009, 2013; Jian Ping et al., 2012; Li Gangzhu et al., 2017; Xue Jianping et al., 2018; Wang Shuqing et al., 2018; Wang Jinfang et al., 2019a, 2020a, 2020b)。这进一步明确了梅劳特乌拉晚石炭世(—早二叠世)蛇绿岩(-洋内弧)北侧,存在晚石炭世奥长花岗岩 TTG 岩石组合和高力罕晚石炭世 TTG 岩带(岩浆弧),反映了与梅劳特乌拉蛇绿岩-洋内弧形成与演化密切相关的晚石炭世 TTG 岩浆事件。

4.3 构造意义

显生宙的英云闪长岩-奥长花岗岩-花岗闪长岩 TTG 岩石组合,代表了显生宙增生型造山带的陆壳增生事件,并在洋陆转换过程的大陆雏体形成中具有重要意义。特别是显生宙的 TTG 岩石组合与前弧玄武岩、高镁安山岩(玻安岩)/高镁闪长岩-镁安山岩、埃达克岩、富铌玄武岩/辉长岩等(洋内弧)岛弧岩浆岩构成的初生弧火成岩构造组合,则代表了新生陆壳生长事件与“大陆雏体”(Sengor et al., 1993; Yogodzinski et al., 1995, 2001; Deng Jinfu et al., 2015a; Xiao Qinghui et al., 2016; Safonova, 2017; Cheng Yang et al., 2019)。二连-贺根山缝合带作为中亚增生型造山带东段构造演化的关键区域之一,广泛发育石炭纪一二叠纪 SSZ 型蛇绿岩-岛弧型岩浆岩组合(图 1),表明了古亚洲洋二连-贺根山洋盆在石炭纪一中二叠世早期仍然处于强烈的大洋

俯冲消减作用阶段。而本文呼都格晚石炭世(306.3 ± 1.9 Ma, 315.5 ± 1.9 Ma)大洋俯冲带岛弧型高铝 TTG 的识别,则表明古亚洲洋二连-贺根山洋盆在晚石炭世正处于洋壳俯冲消减、新生陆壳生长与陆壳侧向增生阶段。本文报道的呼都格晚石炭世大洋俯冲带岛弧型 TTG,在时空分布上与南侧的梅劳特乌拉晚石炭世(—早二叠世)蛇绿岩中前弧玄武岩、高镁安山岩(玻安岩)/高镁闪长岩-镁安山岩、埃达克岩(花岗闪长岩和英云闪长岩等)、富铌玄武岩和富铌辉长岩等构成较为完整的初生弧火成岩构造组合(Deng Jinfu et al., 2015a; Xiao Qinghui et al., 2016; Safonova, 2017; Wang Jinfang et al., 2017a, 2017c, 2018a, 2018b, 2019a, 2020a),形成晚石炭世—早二叠世梅劳特乌拉-高力罕蛇绿岩-TTG 岩带。而且,梅劳特乌拉初生弧火成岩构造组合,可与邻区的迪彦庙蛇绿岩中的早石炭世(—早二叠世)洋内弧火成岩构造组合相类比(Li Yingjie et al., 2012, 2018a, 2018b, 2018c; Cheng Yang et al., 2019, 2020; Wang Jinfang et al., 2020b)。与此同时,Safonova (2017)提出中亚增生型造山带发育洋内弧和 TTG 弧岩浆岩带,并认为发生在洋内弧、陆缘弧的 TTG 岩浆作用为新生陆壳生长的重要地质作用。因此,梅劳特乌拉和迪彦庙初生弧火成岩构造组合的发育和识别,可能揭示古亚洲洋二连-贺根山洋盆在晚石炭世仍然处于(洋内)洋壳俯冲消减、洋内弧 TTG 岩浆活动和新生陆壳生长阶段。

Sengor et al. (1993)提出中亚增生型造山带或阿尔泰型造山带(Altaids)主要由俯冲增生杂岩和岩浆弧所构成,认为大陆地壳主要通过沿大洋俯冲带构造加积作用(形成俯冲增生杂岩)和新生岩浆岩的侵位(形成岩浆弧)而增生,并指出古亚洲洋在三叠纪沿索伦缝合带最终关闭。中亚增生型造山带东段的二连-贺根山缝合带,同样主要由沿俯冲带构造加积作用形成的俯冲增生杂岩和新生岩浆弧所组成。在二连-贺根山缝合带区域内石炭纪一中二叠世早期 SSZ 型蛇绿岩-岛弧岩浆岩出露区,主要发育以下二叠统寿山沟组、大石寨组半深海-深海复理石建造为主的俯冲增生杂岩(Li Yingjie et al., 2012, 2015, 2018a, 2018b, 2018c; Wang Jinfang et al., 2017a, 2017c, 2018a, 2018b; Zhang Qingkui et al., 2018; Cheng Yang et al., 2019)。例如,Zhang Qingkui et al. (2018)提出下二叠统大石寨组由古海沟浊积岩(硅泥质岩、粉砂岩)、岛弧火山岩(变质安山岩、英安岩、流纹岩、火山碎屑岩)和古洋壳残片

(橄榄辉石岩、辉绿岩、枕状玄武岩及部分硅泥质岩)三部分组成,并认为其反映了俯冲带洋壳俯冲与陆壳增生作用。而且,Shang Qinghua (2004)在区内中二叠统哲斯组泥岩中发现放射虫化石,提出哲斯组地层形成于古洋盆环境。Tian Shugang et al. (2016)提出二连-贺根山洋在石炭纪—早二叠世处于古亚洲洋阶段,中二叠世的构造古地理环境逐渐演变为兴蒙海槽阶段。这些研究成果揭示二连-贺根山地区中二叠统哲斯组地层为大洋板块地层或俯冲增生杂岩的重要组成。在梅劳特乌拉-高力罕蛇绿岩-TTG 岩带内,下二叠统寿山沟组和中二叠统哲斯组地层均以俯冲增生杂岩构造楔形体的形式产出。因此,俯冲增生杂岩的发育与识别,从另一个角度揭示该区在晚石炭世—中二叠世处于洋壳俯冲消减、俯冲增生杂岩形成和陆壳增生阶段。

综上所述,作为梅劳特乌拉 高力罕蛇绿岩 TTG 岩带晚石炭世 TTG 岩浆事件的代表性岩石,呼都格 TTG 岩石组合的出现表明古亚洲洋二连 贺根山洋盆在晚石炭世处于洋壳俯冲消减、TTG 岩浆活动与新生陆壳生长的洋陆转换过程中,最终闭合可能在二叠纪末期(Wang Jinfang et al., 2020c, 2020d)。

5 结论

(1)岩石学和岩石地球化学研究表明,呼都格岩体属于高铝 TTG 岩类的 $T_1 T_2 G_1$ 岩石组合,与显生宙 TTG 岩石组合相类似,形成于大洋俯冲带岛弧环境,为岛弧型岩浆岩,是由俯冲洋壳玄武岩脱水部分熔融形成的。

(2)呼都格岩体形成于晚石炭世(306~315.5 Ma),反映了二连-贺根山缝合带晚石炭世大洋俯冲带 TTG 岩浆事件,表明古亚洲洋二连-贺根山洋盆在晚石炭世处于大洋俯冲消减、TTG 岩浆活动和新生陆壳生长的洋陆转换过程中。

References

- Adam John, Rushmer Tracy, O’Neil Jonathan. 2012. Hadean greenstones from the Nuvvuagittuq fold belt and the origin of the Earth’s early continental crust. *Geology*, 40(4):363~366.
- Beard J S. 1991. Dehydration melting and water-saturated melting of basaltic and andesitic greenstones and amphibolites at 1,3, and 6 ~9 kb. *Journal of Petrology*, 32(2):365~401.
- Bourdon E, Eissen J P, Gutscher M A. 2003. Magmatic response to early aseismic ridge subduction: the Ecuadorian margin case (South America). *EPSL*, 205:123~138.
- Chen Bin, Jahn B M, Tian W. 2009. Evolution of the Solonker suture zone constraints from U-Pb ages, Hf isotopic ratios and zircon whol-rock Nd, Sr isotope compositions of subduction-and collision-related magmas and forearc sediments. *Journal of Asian Earth Sciences*, 34(3):245~257.
- Chen Bin, Jahn B M, Wild S, Xu B. 2000. Two contrasting Paleozoic magmatic belts in northern Inner Mongolia, China: protogenesis and tectonic implications. *Tectonophysics*, 328(1~2):157~182.
- Chen Bin, Zhao Guochun, Wilde Sinon. 2001. Subduction and collision-related granitoids from southern Sonidzuqi, Inner Mongolia: isotopic ages and tectonic implication. *Geological Review*, 47(4):361~367(in Chinese with English abstract).
- Cheng Yang, Xiao Qinghui, Li Tingdong, Guo Lingjun, Li Yan, Fan Yuxu, Luo Pengyue, Pang Jinli. 2019. Magmatism and tectonic background of the Early Permian intra-oceanic arc in the Diyanmiao subduction accretion complex belt on the eastern margin of the Central Asian Orogenic Belt. *Earth Science*, 44(06):1879~1891.
- Cheng Yang, Xiao Qinghui, Li Tingdong, Xu Liquan, Mo Lingchao, Li Yan, Fan Yuxu, Guo Lingjun, Pang Jinli. 2020. Discovery of the Carboniferous plagiogranite in the Diyanmiao-Daqing area of West Ujimqin, Inner Mongolia and its implication to the tectonic evolution of the Paleo-Asian Ocean. *Geology and Exploration*, 56(02):302~314 (in Chinese with English abstract).
- Condie K C. 1986. Origin and early growth rate of continents. *Precambrian Research*, 32(4):261~278.
- Condie K C. 2005. TTGs and adakites: are they both slab melts? *Lithos*, 80(1):33~44.
- Corfu F, Hanchar J M, Hoskin P W O. 2003. Atlas of Zircon Textures. *Reviews in Mineralogy & Geochemistry*, 53(1):469~500.
- Defant M J, Drummond M S. 1990. Derivation of some modern arc magmas by melting of young subducted lithosphere. *Nature*, 347(18):662~665.
- Defant J D. 1993. Mount St. Helens; potential example of the partial melting of the subducted lithosphere in a volcanic arc. *Geology*, 21:547~550.
- Deng Jinfu, Feng Yanfang, Di Yongjun, Liu Cui, Xiao Qinghui, Su Shangguo, Zhao Guochun, Meng Fei, Ma Shuai, Yao Tu. 2015a. Magmatic arc and ocean-continent transition; discussion. *Geological Review*, 61(3):473~484 (in Chinese with English abstract).
- Deng Jinfu, Feng Yanfang, Di Yongjun, Liu Cui, Xiao Qinghui, Su Shangguo, Zhao Guochun, Meng Fei, Che Rufeng. 2015b. The intrusive spatial-temporal evolutionary framework in the Paleo-Asian tectonic domain. *Geological Review*, 61(6):1211~1224 (in Chinese with English abstract).
- Deng Jinfu, Liu Cui, Di Yongjun, Feng Yanfang, Xiao Qinghui, Liu Yong, Ding Xiaozhong, Meng Guixiang, Huang Fan, Zhao Guochun, Wu Zongxu. 2018. Discussion on the tonalite-trondhjemite-granodiorite(TTG) petrotectonic assemblage and its subtypes. *Earth Science Frontiers*, 25(06):42~50.
- Drummond M S, Defant M J, Kepezhinskas. 1996. Petrogenesis of slab-derived trondhjemite-tonalite-dacite/adakite magmas. *Trans. Royal Soc. Edinburgh, Earth Sci.*, 87:205~215.
- Fan Yuxu, Li Tingdong, Xiao Qinghui, Cheng Yang, Li Yan, Guo Lingjun, Luo Pengyue. 2019. Zircon U-Pb ages, geochemical characteristics of Late permian granite in West Ujimqin Banner, Inner Mongolia, and tectonic significance. *Geological Review*, 65(01):248~266.
- Feng Yanfang, Deng Jinfu, Xiao Qinghui, Xing Guang, Su Shangguo, Cui Xianyue, Gong Fanying. 2011. Recognizing the TTG rock types; discussion and suggestion. *Geological Journal of China University*, 17(3):406~414 (in Chinese with English abstract).
- Foley S F, Buhre S, Jacob D E. 2003. Evolution of the Archaean crust by delamination and shallow subduction. *Nature*, 421(6920):249~252.
- Foley S, Tiepolo M and Vannucci R. 2002. Growth of early continental crust controlled by melting of amphibolite in

- subduction zones. *Nature*, 417(6891):837~840.
- Hawkesworth C J, Dhuime B, Pietranik A B. 2010. The generation and evolution of the continental crust. *Journal of the Geological Society*, 167(2):229~248.
- Jian Ping, Liu D Y, Kröner A. 2010. Evolution of a Permian intraoceanic arc-trench system in the Solonker suture zone, Central AsianOrogenic Belt, China and Mongolia. *Lithos*, 118: 169~190.
- Jian Ping, Kröner A, Windley B F, Shi Yuruo, Zhang Wei, Zhang Liqiao, Yang Weiran. 2012. Carboniferous and Cretaceous mafic-ultramafic massifs in Inner Mongolia (China): A SHRIMP zircon and geochemical study of the previously presumed integral“Hegenshan ophiolite”. *Lithos*, 142~143:48 ~66.
- Jiang Yang, Zhao Xilin, Lin Shoufa, Davis D W, Xing Guangfu, Li Longming, Duan Zheng. 2014. Identification and tectonic implication of Neoproterozoic continental margin-arc TTG assemblage in Southeastern margin of the Yangtze carton. *Acta Geological Sinica*, 88(8):1461~1474 (in Chinese with English abstract).
- Kang Jianli, Xiao Zhibin, Wang Huichu. 2016. Late Paleozoic Subduction of the Paleo-Asian Ocean: geochronological and geochemical evidence from the meta-basic volcanics of Xilinhhot, Inner Mongolia. *Acta Geologica Sinica*, 90(2):383~397.
- Li Gangzhu, Wang Yujing, Li Chengyuan. 2017. Discovery of Early Permian radiolarian fauna in the Solon Obo ophiolite belt, Inner Mongolia and its geological significance. *Chin Sci Bull*, 62(05): 400~406(in Chinese without English abstract).
- Li Jinyi, Gao Liming, Sun Guihua, Li Yaping, Wang Yanbin. 2007. Shuangjingzi Middle Triassic syn-collisional crust derived granite in the East Inner Mongolia and its constraint on the timing of collision between Siberian and Sino Korean paleoplates. *Acta Petrologica Sinica*, 23 (03): 565 ~ 582 (in Chinese with English abstract).
- Liu Jianfeng, Chi Xiaoguo, Zhang Xingzhou, Ma Zhihong, Zhao Zhi, Wang Tiefu, Hu Zhaochu, Zhao Xiuyu. 2009. Geochemical characteristic of Carboniferous quartz-diorite in the Southern Xiuwu area, Inner Mongolia and Its tectonic significance. *Acta Geologica Sinica*, 83(3):365~376(in Chinese with English abstract).
- Liu Jianfeng, Li Jinyi, Chi Xiaoguo, Qu Junfeng, Hu Zhaochu, Fang Shu, Zhang Zhong. 2013. A late-Carboniferous to early early-Permian subduction-accretion complex in Daqing pasture, southeastern Inner Mongolia: Evidence of northward subduction beneath the Siberian paleoplate southern margin. *Lithos*, 177 (2):285~296.
- Liu Jianhui, Liu Fulai, Ding Zhengjiang, Liu Pinghua, Wang Fang. 2015. Early Precambrian major magmatic events, and growth and evolution of continental crust in the Jiaobei terrane, North China Craton. *Acta Petrologica Sinica*, 31(10):2942~2958 (in Chinese with English abstract).
- Liu Rui, Yang Zhen, Xu Qidong, Zhang Xiaojun, Yao Chunliang. 2016. Zircon U-Pb ages, elemental and Sr-Nd- Pb isotopic geochemistry of the Hercynian granitoids from the southern segment of the Da Hinggan Mts.: petrogenesis and tectonic implications. *Acta Petrologica Sinica*, 32(05):1505 ~ 1528 (in Chinese with English abstract).
- Li Yingjie, Wang Jinfang, Li Hongyang, Dong Peipei. 2012. Recognition of Diyanmiao ophiolite in Xi Ujimqin Banner, Inner Mongolia. *Acta Petrologica Sinica*, 28 (4): 1282 ~ 1290 (in Chinese with English abstract).
- Li Yingjie, Wang Jinfang, Li Hongyang and Dong Peipei. 2015. Recognition of Meilaotewula ophiolite in Xi Ujimqin Banner, Inner Mongolia. *Acta Petrologica Sinica*, 31(5):1461~1470(in Chinese with English abstract).
- Li Yingjie, Wang Jinfang, Wang Genhou, Dong Peipei, Li Hongyang, Hu Xiaojia. 2018a. Discovery of the plagiogranites in the Diyanmiao ophiolite, Southeastern Central Asian Orogenic Belt, Inner Mongolia, China and Its Tectonic Significance. *Acta Geologica Sinica(English Edition)*, 92(02):568~585.
- Li Yingjie, Wang Jinfang, Li Hongyang and Dong Peipei. 2018b. Discovery and significance of the Dahate fore-arc basalts from Diyanmiao ophiolite in Inner Mongolia. *Acta Petrologica Sinica*, 34(2):469~482(in Chinese with English abstract).
- Li Yingjie, Wang Genhou, Santosh M, Wang Jinfang, Dong Peipei, Li Hongyang. 2018c. Supra-subduction zone ophiolites from Inner Mongolia, North China: Implications for the tectonic history of the southeastern Central Asian Orogenic Belt. *Gondwana Research*, 59:126~143.
- Ludwig K R. 2003. User's Manual for Isoplot 3. 00: A Geochronological Toolkit For Microsoft Excel. Berkeley C A: Berkeley Geochronology Center, Special Publication, 4:1~71.
- Martin H, Smithies R H, Rapp R, Moyen J F. 2005. An overview of adakite, tonalite-trondhjemite-granodiorite (TTG), and sanukitoid: Relationships and some implications for crustal evolution. *Lithos*, 79(1~2):1~24.
- Martin H. 1987. Petrogenesis of Archaean trondhjemites, tonalites, and granodiorites from Eastern Finland: Major and trace element geochemistry. *Journal of Petrology*, 28(5):921~953.
- Martin H. 1999. Adakitic magmas; modern analogues of Archaean granitoids. *Lithos*, 46: 411~429.
- Miao Laicheng, Fan W M, Liu D Y. 2008. Geochronology and geochemistry of the Hegenshan ophiolitic complex: implications for late-stage tectonic evolution of the Inner Mongolia-Daxinganling Orogenic Belt, China. *Journal of Asian Earth Sciences*, 32(5~6):348~370.
- Middlemost E A K. 1994. Naming materials in the magma/igneous rock system. *Earth-Science Reviews*, 37:215~224.
- O'Connor J T. 1965. A classification for quartz-rich igneous rocks based on feldspar ratios. *U. S. Geol. Surv. Prof. Paper*, 525-B:79~84.
- Pearce J A, Harris N B W, Tindle A G. 1984. Trace element discrimination diagrams for the tectonic interpretation of granitic rocks. *Journal of Petrology*, 25(4),956~983.
- Peccerillo A, Taylor S R. 1976. Geochemistry of ecocene calc-alkaline volcanic rocks from the Kastamonu Area, Northern Turkey. *Contributions to Mineralogy and Petrology*, 58:63~81.
- Rapp R P, Watson E B, Miller C F. 1991. Partial melting of amphibolite eclogite and the origin of Archean trondhjemites and tonalites. *Precambrian Research*, 51(1~4):1~25.
- Rapp R P, Watson E B. 1995. Dehydration melting of metabasalt at 8 ~ 32kbar: implications for continental growth and crust-mantle recycling. *Journal of Petrology*, 36:891~931.
- Rapp R P, Shimizu N, Norman M D. 1999. Reaction between slab-derived melts and peridotite in the mantle wedge: experimental constraints at 3.8GPa. *Chemical Geology*, 160(4):335~356.
- Rapp R P, Shimizu N and Norman M D. 2003. Growth of early continental crust by partial melting of eclogite. *Nature*, 425 (6958):605~609.
- Safanova I. 2017. Juvenile versus recycled crust in the Central Asian Orogenic belt: implications from ocean plate stratigraphy, blueschist belts and intra-oceanic arcs. *Gondwana Research*, 47:6~27.
- Samaniego P, Martin H, Robin C. 2002. Transition from talc-alkalic to adakitic magmatism at Cayambe volcano, Ecuador: insights into slab melts and mantle wedge interactions. *Geological Society of America*, 30(11):967~970.
- Sengor A M C, Natalin B A, Burtman V S. 1993. Evolution of the Altaiid tectonic collage and Paleozoic crustal growth in Eurasia. *Nature*, 364:299~307.
- Shang Qinghua. 2004. The discovery and significance of Permian radiolarians Northern Orogenic belt in the northern and middle Inner Mongolia. *Chinese Science Bulletin*, 49:2574~2579.
- Shi Yuruo, Liu Cui, Deng Jinfu, Jian Ping. 2014. Geochronological frame of granitoids from Central Inner Mongolia and its tectonomagmatic evolution. *Acta Petrologica Sinica*, 30 (11): 3155~3171(in Chinese with English abstract).
- Smithies R H, Champion D C, Van Kranendonk M J. 2009.

- Formation of Paleoarchean continental crust through infracrustal melting of enriched basalt. *Earth and Planetary Science Letters*, 81(3):298~306.
- Stern C R, Killian R. 1996. Role of the subducted slab, mantle wedge and continental crust in the generation of adakites from the Andean Austral Volcanic Zone. *Contrib. Mineral. Petrol.*, 123:263~281.
- Sun S S, McDonough W F. 1989. Chemical and Isotope Systematics of Oceanic Basalts: Implications for Mantle Composition and Processes. *Geological Society of London, Special Publication*, 42:313~345.
- Thorkelson D J, Breitsprecher K. 2005. Partial melting of slab window margins: genesis of adakitic and non-adakitic magmas. *Lithos*, 79:24~41.
- Tian Shugang, Li Zishun, Zhanu Yongsheng, Gonu Yuexuan, Zhai Daxing, Wand Meng. 2016. Late Carboniferous-Permian tectono-geographical conditions and development in Eastern Inner Mongolia and adjacent areas. *Acta Geologica Sinica*, 90(04):688~707(in Chinese with English abstract).
- Viruete J E, Contreras F, Stein C. 2007. Magmatic relationships and ages between adakites, magnesian andesites and Nb-enriched basalt-andesites from Hispaniola: record of a major change in the Caribbean island arc magma sources. *Lithos*, 99(3~4):151~177.
- Wang Cheng, Ren Limin, Zhang Xiaojun, Yu Guofei, Fang Lei. 2019. Discovery and significance of the fore-arc basalts from the Chonggengshan ophiolite in Inner Mongolia. *Geological Science and Technology Information*, 38(03):1~11(in Chinese with English abstract).
- Wang Hui, Wang Yujing, Chen Zhiyong, Li Yuxi, Su Maorong, Bai Libing. 2005. Discovery of the Permian Radiolarians from the Bayanaobao area, Inner Mongolia. *Journal of Stratigraphy*, 29(4):368~372(in Chinese with English abstract).
- Wang Jinfang, Li Yingjie, Li Hongyang, Dong Peipei. 2017a. Discovery of Early Permian intra-oceanic arc adakite in the Meilaotewula ophiolite, Inner Mongolia and its evolution model. *Acta Geologica Sinica*, 91(08):1776~1795(in Chinese with English abstract).
- Wang Jinfang, Li Yingjie, Li Hongyang, Dong Peipei. 2017b. LA-ICP-MS zircon U-Pb dating of the Nuhete Early Cretaceous A-type granite in Xi Ujimqin Banner of Inner Mongolia and its geological significance. *Geological Bulletin of China*, 36(8):1343~1358(in Chinese with English abstract).
- Wang Jinfang, Li Yingjie, Li Hongyang. 2017c. Zircon LA-ICP-MS U-Pb age and island-arc origin of the Bayanhua gabbro in the Hegenshan Suture Zone, Inner Mongolia. *Acta Geologica Sinica (English Edition)*, 91(6):2316~2317.
- Wang Jinfang, Li Yingjie, Li Hongyang, Dong Peipei. 2018a. The discovery of the Early Permian high-Mg diorite in Meilaotewula SSZ ophiolite of Inner Mongolia and its intra-oceanic subduction. *Geology in China*, 45(4):706~719(in Chinese with English abstract).
- Wang Jinfang, Li Yingjie, Li Hongyang, Dong Peipei. 2018b. Zircon U-Pb dating of the Wulangou adakite, Inner Mongolia and its tectonic setting. *Geological Bulletin of China*, 37(10):1933~1943(in Chinese with English abstract).
- Wang Jinfang, Li Yingjie, Li Hongyang, Dong Peipei. 2019a. Zircon U-Pb ages and geochemical characteristics of the Baiyinhushu trondjemite in the Hegenshan suture zone and their tectonic implications. *Geological Review*, 65(04):857~872(in Chinese with English abstract).
- Wang Jinfang, Li Yingjie, Li Hongyang, Dong Peipei. 2019b. Post-orogeny of the Hegenshan suture zone: zircon U-Pb age and geochemical constraints from volcanic rocks of the Manketouebo Formation. *Geological Bulletin of China*, 38(09):1443~1454(in Chinese with English abstract).
- Wang Jinfang, Li Yingjie, Li Hongyang, Dong Peipei. 2020a. Late Carboniferous intraoceanic subduction of the Paleo — Asian Ocean: New evidence from the Zagayin high-Mg andesite in the Meilaotewula SSZ ophiolite. *Geological Review*, 66(02):289~306 (in Chinese with English abstract).
- Wang Jinfang, Li Yingjie, Li Hongyang, Dong Peipei. 2020b. Intra-oceanic subduction of the Paleo-Asian Oceanic slab: New evidence from the Early Carboniferous quartz diorite in the Diyanmiao ophiolite. *Acta Geologica Sinica(English Edition)*, 94(02):565~567.
- Wang Jinfang, Li Yingjie, Li Hongyang, Dong Peipei. 2020c. Zircon U-Pb Dating, geochemistry and tectonic implication of the Artala Middle Triassic A-type granite in Inner Mongolia. *Geological Bulletin of China*, 39(01):51~61 (in Chinese with English abstract).
- Wang Jinfang, Li Yingjie, Li Hongyang, Dong Peipei. 2020d. Paleo-Asian Ocean subducted slab breakoff and post orogenic extension: evidence from geochronology and geochemistry of volcanic rocks in the Hegenshan suture zone. *Acta Geologica Sinica*, 94(12):3561~3580 (in Chinese with English abstract).
- Wang Shuqing, Hu Xiaojia, Yang Zeli, Zhao Hualei, Zhang Yong, Hao Shuang, He Li. 2018. Geochronology, geochemistry, Sr-Nd-Hf isotopic characteristics and geological significance of Carboniferous Yuejin arc intrusive rocks of Xilinhot, Inner Mongolia. *Earth Science*, 43(3):1~31(in Chinese with English abstract).
- Windley B F, Alexeev D, Xiao W J, Krner F, Badarch G. 2007. Tectonic models for accretion of the Central Asian Orogenic Belt. *Journal of the Geological Society*, 164(1):31~47.
- Wu Mingqian, Zuo Menglu, Zhang Dehui, Zhao Guochun. 2014. Genesis and Diagenetic Environment of TTG Suite. *Geological Review*, 60(3):503~514(in Chinese with English abstract).
- Wu Yuanbao, Zheng Yongfei. 2004. Genesis of zircon and its constraints on interpretation of U-Pb age. *Chinese Science Bulletin*, 49(15):1554~1569.
- Xiao Qinghui, Li Tingdong, Pan Guitang. 2016. Petrologic ideas for identification of ocean-continent transition: Recognition of intra-oceanic arc and initial subduction. *Geology in China*, 43(3):721~737(in Chinese with English abstract).
- Xiao Wenjiao, Windley B F, Hao Jie. 2003. Accretion leading to collision and the Permian Solonker suture, Inner Mongolia, China: Termination of the central Asian orogenic belt. *Tectonics*, 22(6):1069~1089.
- Xiao Wenjiao, Windley B F, Huang B C. 2009. End-Permian to mid-Triassic termination of the accretionary processes of the southern Altaids; implications for the geodynamic evolution, Phanerozoic continental growth, and metallogeny of Central Asia. *Int. J. Earth Sci.*, 98:1189~1217.
- Xiong X L. 2006. Trace element evidence for growth of early continental crust by melting of rutile-bearing hydrous eclogite. *Geology*, 34(11):945~948.
- Xue Jianping, Liu Meiyu, Li Gangzhu, Zhao Guangming. 2018. Zircon geochronology and geochemistry of Haer Bogetuoer TTG rock, Solonker zone, Inner Mongolia and their tectonic implications. *Earth Science Frontiers*, 25(3):230~239 (in Chinese with English abstract).
- Yogodzinski G M, Lees J M, Churikova T G. 2001. Geochemical evidence for the melting of subducting oceanic lithosphere at plate edges. *Nature*, 409(6819):500~504.
- Yogodzinski G M, Kay R W, Volynets O N. 1995. Magnesian andesites in the western Aleutian Komandorsky region: implication for slab melting and pressures in the mantle wedge. *Geological Society of America Bulletin*, 107:505~519.
- Zhang Qi, Zhai M G. 2012. What is the Archean TTG? *Acta Petrologica Sinica*, 28(11):3446~3456 (in Chinese with English abstract).
- Zhang Qingkui, Yang Bin, Shao Xuefeng, Chen Shuliang, Zhao Mingyuan, Lü Fengxiang. 2018. The petrological characteristics and tectonic implications of turbidite and seismite in Balagedai tectonic melange belt, Inner Mongolia: Take regional geological survey scaled 1:50000 in Halahei area, Inner Mongolia as an example. *Geological Bulletin of China*, 7(09):1731~1735 (in Chinese with English abstract).

Chinese with English abstract).

Zhang Xiaofei, Zhou Yi, Cao Jun, Teng Chao. 2018. Geochronological and geochemical features of bimodal intrusive rocks in the Hanwula area of Xiwu Banner, Inner Mongolia: constraints on closure of the Paleo-Asian Ocean. *Acta Geologica Sinica*, 92(4): 665~686 (in Chinese with English abstract).

参 考 文 献

- 陈斌,赵国春,Simon Wilde. 2001. 内蒙古苏尼特左旗南两类花岗岩同位素年代学及其构造意义. 地质论评, 47(4): 361~367.
- 程杨,肖庆辉,李廷栋,郭灵俊,李岩,范玉须,罗鹏跃,庞进力. 2019. 中亚造山带东缘迪彦庙俯冲增生杂岩带早二叠世洋内弧岩浆作用及构造背景. 地球科学, 44(06): 1879~1891.
- 程杨,肖庆辉,李廷栋,许立权,莫凌超,李岩,范玉须,郭灵俊,庞进力. 2020. 西乌旗迪彦庙-达青地区石炭纪斜长花岗岩的发现及其对古亚洲洋构造演化的指示意义. 地质与勘探, 56(02): 302~314.
- 邓晋福,冯艳芳,狄永军,刘翠,肖庆辉,苏尚国,赵国春,孟斐,马帅,姚图. 2015a. 岩浆弧火成岩构造组合与洋陆转换. 地质论评, 61(03): 473~484.
- 邓晋福,冯艳芳,狄永军,刘翠,肖庆辉,苏尚国,赵国春,孟斐,车如风. 2015b. 古亚洲构造域侵入岩时-空演化框架. 地质论评, 61(6): 1211~1224.
- 邓晋福,刘翠,狄永军,冯艳芳,肖庆辉,刘勇,丁孝忠,孟贵祥,黄凡,赵国春,吴宗絮. 2018. 英云闪长岩-奥长花岗岩-花岗闪长岩(TTG)岩石构造组合及其亚类划分. 地学前缘, 25(06): 42~50.
- 范玉须,李廷栋,肖庆辉,程杨,李岩,郭灵俊,罗鹏跃. 2019. 内蒙古西乌珠穆沁旗晚二叠世花岗岩的锆石U-Pb年龄、地球化学特征及其构造意义. 地质论评, 65(01): 248~266.
- 冯艳芳,邓晋福,肖庆辉,邢光福,苏尚国,崔显岳,公凡影. 2011. TTG岩类的识别:讨论与建议. 高校地质学报, 17(3): 406~414.
- 姜扬,赵希林,林寿发,DAVIS D W,邢光福,李龙明,段政. 2014. 扬子克拉通东南缘新元古代陆缘弧型TTG的厘定及其构造意义. 地质学报, 88(8): 1461~1474.
- 康健丽,肖志斌,王惠初. 2016. 内蒙古锡林浩特早石炭世构造环境:来自变质基性火山岩的年代学和地球化学证据. 地质学报, 90(2): 383~397.
- 李钢柱,王玉净,李成元. 2017. 内蒙古索伦山蛇绿岩带早二叠世放射虫动物群的发现及其地质意义. 科学通报, 62(05): 400~406.
- 李锦铁,高立明,孙桂华,李亚萍,王彦斌. 2007. 内蒙古东部双井子中三叠世同碰撞壳源花岗岩的确定及其对西伯利亚与中朝古板块碰撞时限的约束. 岩石学报, 023(03): 565~582.
- 李英杰,王金芳,李红阳,董培培. 2012. 内蒙古西乌旗迪彦庙蛇绿岩的识别. 岩石学报, 28(4): 1282~1290.
- 李英杰,王金芳,李红阳,董培培. 2015. 内蒙古西乌旗梅劳特乌拉蛇绿岩的识别. 岩石学报, 31(5): 1461~1470.
- 李英杰,王金芳,王根厚,李红阳,董培培. 2018b. 内蒙古迪彦庙蛇绿岩带达哈特前弧玄武岩的发现及其地质意义. 岩石学报, 34(2): 469~482.
- 刘建峰,迟效国,张兴洲,马志红,赵芝,王铁夫,胡兆初,赵秀羽. 2009. 内蒙古西乌旗南部石炭纪石英闪长岩地球化学特征及其构造意义. 地质学报, 83(3): 365~376.
- 刘建辉,刘福来,丁正江,刘平华,王舫. 2015. 胶北地体早前寒武纪重大岩浆事件、陆壳增生及演化. 岩石学报, 31(10): 2942~2958.
- 刘锐,杨振,徐启东,张晓军,姚春亮. 2016. 大兴安岭南段海西期花岗岩类锆石U-Pb年龄、元素和Sr-Nd-Pb同位素地球化学:岩石成因及构造意义. 岩石学报, 32(05): 1505~1528.
- 石玉若,刘翠,邓晋福,简平. 2014. 内蒙古中部花岗质岩类年代学格架及该区构造岩浆演化探讨. 岩石学报, 30(11): 3155~3171.
- 田树刚,李子舜,张永生,宫月萱,翟大兴,王猛. 2016. 内蒙东部及邻区晚石炭世-二叠纪构造古地理环境及演变. 地质学报, 90(04): 688~707.
- 王成,任利民,张晓军,余国飞,方磊. 2019. 内蒙古崇根山蛇绿岩前弧玄武岩的发现及其地质意义. 地质科技情报, 38(03): 1~11.
- 王惠,王玉净,陈志勇,李玉玺,苏茂荣,白立兵. 2005. 内蒙古巴彦敖包二叠纪放射虫化石的发现. 地层学杂志, 29(4): 368~372.
- 王金芳,李英杰,李红阳,董培培. 2017a. 内蒙古梅劳特乌拉蛇绿岩中埃达克岩的发现及其演化模式. 地质学报, 91(08): 1776~1795.
- 王金芳,李英杰,李红阳,董培培. 2017b. 内蒙古西乌旗努和特早白垩世A型花岗岩LA-ICPMS锆石U-Pb年龄及其地质意义. 地质通报, 36(8): 1343~1358.
- 王金芳,李英杰,李红阳,董培培. 2018a. 内蒙古梅劳特乌拉蛇绿岩中早二叠世高镁闪长岩的发现及洋内俯冲作用. 中国地质, 45(4): 706~719.
- 王金芳,李英杰,李红阳,董培培. 2018b. 内蒙古乌兰沟埃达克岩锆石U-Pb年龄及构造环境. 地质通报, 37(10): 1933~1943.
- 王金芳,李英杰,李红阳,董培培. 2019a. 贺根山缝合带白音呼舒奥长花岗岩锆石U-Pb年龄、地球化学特征及构造意义. 地质论评, 65(04): 857~872.
- 王金芳,李英杰,李红阳,董培培. 2019b. 内蒙古贺根山缝合带后造山作用——满克头鄂博组火山岩锆石U-Pb年龄和地球化学制约. 地质通报, 38(09): 1443~1454.
- 王金芳,李英杰,李红阳,董培培. 2020a. 古亚洲洋晚石炭世俯冲作用:梅劳特乌拉蛇绿岩中扎嘎音高镁安山岩证据. 地质论评, 66(02): 289~306.
- 王金芳,李英杰,李红阳,董培培. 2020c. 内蒙古阿尔塔拉中三叠世A型花岗岩锆石U-Pb年龄、地球化学特征及构造意义. 地质通报, 39(01): 51~61.
- 王金芳,李英杰,李红阳,董培培. 2020d. 古亚洲洋俯冲板片断离与后造山伸展:贺根山缝合带火山岩年代学和地球化学证据. 地质学报, 94(12): 3561~3580.
- 王树庆,胡晓佳,杨泽黎,赵华雷,张永,郝爽,何丽. 2018. 兴蒙造山带中段锡林浩特跃进地区石炭纪岛弧型侵入岩年代学、地球化学、Sr-Nd-Hf同位素特征及其地质意义. 地球科学, 43(3): 1~31.
- 吴鸣谦,左梦璐,张德会,赵国春. 2014. TTG岩套的成因及其形成环境. 地质论评, 60(3): 503~514.
- 肖庆辉,李廷栋,潘桂棠. 2016. 识别洋陆转换的岩石学思路-洋内弧与初始俯冲的识别. 中国地质, 43(3): 721~737.
- 薛建平,刘美玉,李钢柱,赵广明. 2018. 内蒙古索伦山地区哈尔博格托尔TTG岩锆石年代学、岩石地球化学及大地构造意义. 地学前缘, 25(3): 230~239.
- 张旗,翟明国. 2012. 太古宙TTG岩石是什么含义? 岩石学报, 28(11): 3446~3456.
- 张庆奎,杨宾,邵学峰,陈树良. 2018. 内蒙古巴拉格歹地区构造混杂岩带中浊积岩、震积岩特征及意义——内蒙古哈拉黑等八幅1:5万区域地质调查为例. 地质通报, 7(09): 1731~1735.
- 张晓飞,周毅,曹军,滕超,王必任,张华川,冯俊岭,刘俊来. 2018. 内蒙古西乌旗罕乌拉地区双峰式侵入体年代学、地球化学特征及其对古亚洲洋闭合时限的制约. 地质学报, 92(4): 665~686.

Late Carboniferous TTG magmatic event in the Hegenshan suture zone: zircon U-Pb geochronology and geochemical constraints from the Huduge trondhjemite

WANG Jinfang*, LI Yingjie, LI Hongyang, DONG Peipei

College of the Earth Sciences, Hebei GEO University, Shijiazhuang, Hebei, 050031

* Corresponding author: wjfb1983@163.com

Abstract

The TTG magmatic event was an important geological process for the juvenile crustal growth. The Huduge trondhjemite is located in the Meilaotewula SSZ type ophiolite of the Hegenshan suture zone in the Xi Ujimqin Banner of Inner Mongolia. We present results of field geological survey, petrology, geochemistry and zircon U Pb geochronology to discuss the petrogenesis, tectonic setting, the TTG magmatic event and the final closure time subduction process of the Erenhot Hegenshan ocean basin (EHOB) of the Paleo Asian Ocean (PAO). Petrogeochemical studies show that the Huduge pluton has high SiO_2 (66.27%~71.59%), Al_2O_3 (15.23%~15.94%), Na_2O (4.13%~6.59%), Sr (196.60×10^{-6} ~ 465.40×10^{-6}) and low K_2O (1.72%~2.53%), Y (5.70×10^{-6} ~ 12.63×10^{-6}) contents, is enriched in Ba, Sr large ion lithophile elements and LREE, and depleted in Nb, Ta, Ti, P high field strength elements and HREE. There is no pronounced Eu anomaly. The lithological and geochemical characteristics show that the Huduge pluton belongs to tonalite trondhjemite granodiorite (TTG) assemblages dominated by trondhjemite. The geochemical characteristics of the TTG assemblages are similar to those of high SiO_2 adakites except for the relatively low Sr, Mg, Ni, Cr content. The TTG was probably formed in island arc setting of oceanic subduction zone and comprises of island arc magmatic rocks. It is inferred that the TTG might have been derived from the dehydration melting of the subducted oceanic crust. The zircon U Pb LA ICP MS dating provides two formation ages: 306.3 ± 1.9 Ma and 315.5 ± 1.9 Ma, indicating that the pluton was emplaced in the Late Carboniferous, reflecting the TTG magmatism and juvenile crustal growth events of oceanic subduction zone in the Hegenshan suture zone during the Late Carboniferous. Based on the petrotectonic assemblage of the fore arc basalts, high Mg andesite/high Mg diorite, high SiO_2 adakites, TTG and Nb enriched basalt/gabbro in the Meilaotewula Gaolian ophiolite TTG belt, it is suggested that while the EHOB of the PAO may have been in the ocean continent transition process of oceanic subduction, TTG magmatism and juvenile crustal growth occurred in the Late Carboniferous.

Key words: trondhjemite; TTG; Late Carboniferous; ocean continent transition; Hegenshan suture zone